



Article

Anticancer and Antiphytopathogenic Activity of Fluorinated Isatins and Their Water-Soluble Hydrazone Derivatives

Andrei V. Bogdanov ^{1,*†}, Margarita Neganova ^{1,2,†}, Alexandra Voloshina ¹, Anna Lyubina ¹, Syumbelya Amerhanova ¹, Igor A. Litvinov ¹, Olga Tsivileva ³, Nurgali Akylbekov ⁴, Rakhmetulla Zhapparbergenov ^{4,*}, Zulfia Valiullina ⁵, Alexandr V. Samorodov ⁵ and Igor Alabugin ^{1,6}

- ¹ Arbuzov Institute of Organic and Physical Chemistry, FRC Kazan Scientific Center, Russian Academy of Sciences, Akad. Arbuzov St. 8, Kazan 420088, Russia; neganovam@ipac.ac.ru (M.N.); microbi@iopc.ru (A.V.); aplyubina@gmail.com (A.L.); syumbelya07@mail.ru (S.A.); litvinov@iopc.ru (I.A.L.); ialabugin@gmail.com (I.A.)
- ² Institute of Physiologically Active Compounds at Federal Research Center of Problems of Chemical Physics and Medicinal Chemistry, Russian Academy of Sciences, Severnij Pr. 1, Chernogolovka 142432, Russia
- ³ Institute of Biochemistry and Physiology of Plants and Microorganisms, Saratov Scientific Centre of the Russian Academy of Sciences, Entuziastov Ave. 13, Saratov 410049, Russia; tsivileva_o@ibppm.ru
- ⁴ Laboratory of Engineering Profile “Physical and Chemical Methods of Analysis”, Korkyt Ata Kyzyldorda University, Aitekebie Str. 29A, Kyzyldorda 120014, Kazakhstan; nurgali_089@mail.ru
- ⁵ Department of Pharmacology, Bashkir State Medical University, Lenin St. 8, Ufa 450008, Russia; z_suleimanova@mail.ru (Z.V.); avsamorodov@gmail.com (A.V.S.)
- ⁶ Department of Chemistry and Biochemistry, Florida State University, 95 Chieftan Way, Tallahassee, FL 32306-4390, USA
- * Correspondence: abogdanov@inbox.ru (A.V.B.); ulagat-91@mail.ru (R.Z.); Tel.: +7-843-272-7384 (A.V.B.); +7-724-223-1041 (R.Z.)
- † These authors contributed equally to this work.



Citation: Bogdanov, A.V.; Neganova, M.; Voloshina, A.; Lyubina, A.; Amerhanova, S.; Litvinov, I.A.; Tsivileva, O.; Akylbekov, N.; Zhapparbergenov, R.; Valiullina, Z.; et al. Anticancer and Antiphytopathogenic Activity of Fluorinated Isatins and Their Water-Soluble Hydrazone Derivatives. *Int. J. Mol. Sci.* **2023**, *24*, 15119. <https://doi.org/10.3390/ijms242015119>

Academic Editors: Nam Deuk Kim and Bernhard Biersack

Received: 4 August 2023

Revised: 5 October 2023

Accepted: 6 October 2023

Published: 12 October 2023



Copyright: © 2023 by the authors. Licensee MDPI, Basel, Switzerland. This article is an open access article distributed under the terms and conditions of the Creative Commons Attribution (CC BY) license (<https://creativecommons.org/licenses/by/4.0/>).

1. Introduction

The isatin heterocyclic system is the precursor of a large number of derivatives [1,2] with a wide range of biological and pharmacological properties [3–6]. A number of properties reported for this class of compounds include anticonvulsant [7,8], antistress and anxiogenic [9], antiviral [10], antimicrobial [11], antituberculous [12], antimalarial [13], antifungal [14], and antibacterial [15], which determine their main areas of use. Among the many pharmacological or medical applications of isatin and its derivatives (Figure 1), their use as antitumor agents deserves special attention. Several isatin derivatives have already passed clinical trials and have become approved anticancer drugs [16]. In particular, the

most promising isatin derivative, sunitinib, has been clinically approved by the FDA for the treatment of gastrointestinal stromal tumors, renal cell carcinoma, and a rare type of pancreatic cancer [17]. However, efforts are continuing to diversify chemical modifications and achieve deeper insights into the mechanism of biological action of isatin derivatives. Further rational research is needed to create more effective drugs with less systemic toxicity, better pharmacological characteristics, and a clear mechanism of action.

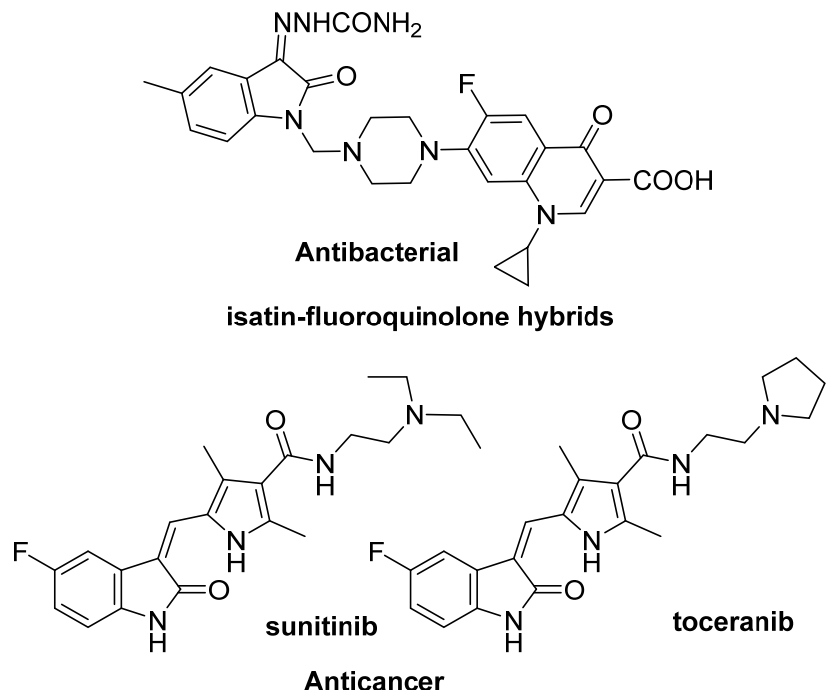


Figure 1. Fluorinated isatin derivatives exhibit various types of biological activity.

One of the limiting factors in the medical and biological applications of many isatin derivatives is their low water solubility. One approach to solving this problem is based on the introduction of an ammonium moiety. Not only does this positively charged group improve the desired physicochemical characteristics, but it can also expand the range of action of the compounds. This is evidenced by recent reviews on the therapeutic possibilities of various quaternary ammonium compounds [18–22]. Earlier, we also demonstrated the high potential of isatin hydrazones containing a quaternary ammonium center in the search for drug candidates for combating human and plant diseases [23–27] (Figure 2).

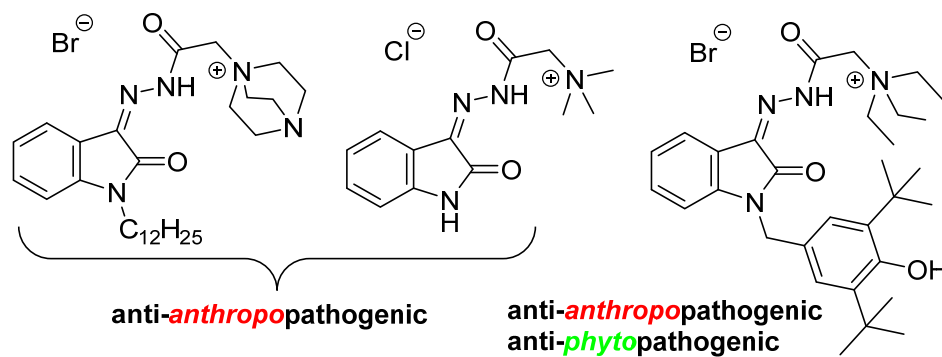


Figure 2. Isatin-3-acylhydrazones possess antimicrobial activity.

Another advantage of isatins as a promising platform for the design and development of new drugs is the possibility of introducing additional substituents at positions of the isatin ring. One of the popular approaches to chemical modifications is the introduction of

halogen atoms. For example, approximately 25–30% of new drugs on the market contain at least one fluorine atom [28]. This modification often leads to a significant increase in an existing type of biological activity and/or an expansion of the action spectrum [29].

In numerous systematic reviews and meta-analyses, there is a large amount of evidence that excessive platelet count contributes to the progression of malignant neoplasms [30–32]. This is due to the formation of specific interactions between platelets and neoplastic cells, which leads to increased survival of tumor cells in the bloodstream, increased spread of tumor foci, and, as a result, metastasis in places remote from the primary occurrence [33]. In this regard, considerable attention of researchers is focused on the use of the well-known anticoagulants as adjunctive therapy for oncological diseases, which is an irreversible inhibitor of platelet cyclooxygenase [34], and a number of clinical studies have demonstrated its positive clinical effects in the treatment of prostate cancer [35], mammary glands [36], stomach [37], etc. That is why the presence of antiplatelet properties as a mechanism of action for potential antitumor agents is considered a promising approach to the development of therapeutic agents to combat oncopathologies.

Various modifications of isatin molecules can lead to the appearance of different desired properties. For example, phosphate derivatives of isatin hydrazones have been shown to have higher activity against sugar cane phytopathogenic fungi than some currently used synthetic fungicides [38]. Evaluation of the fungicidal activity of dialkylphosphorylhydrazones showed that several compounds are able to effectively inhibit the growth of *Rhizoctonia solani* and *Fusarium oxysporum*. In addition, these compounds did not interfere with the germination of lettuce seeds, which indicates the absence of phytotoxicity and makes them potential leaders in the search for new fungicides [39].

Complexation of several compounds with isatin was demonstrated to yield good antibacterial potential, frequently based on the synergic effects of isatin combinations against selected microorganisms [40]. The current list of bacterial pathogens isolated from various crop plants and commonly grown vegetables frequently comprises *Micrococcus luteus*, *Pseudomonas fluorescens*, *Pectobacterium carotovorum* (*Erwinia carotovora*), *Xanthomonas campestris*, and *Pectobacterium atrosepticum* (*Erwinia carotovora* subsp. *atrosepticum*) [41–43]. The top five cereal bacterial pathogens on the list include *Pseudomonas* and *Xanthomonas* [44].

Fungal pathogens cause 70–80% of all plant diseases [45], possessing the potential to cause large-scale disease outbreaks in a very limited period of time. Damage from these pathogens results in the destruction of the roots until the entire plant dies and in the eventual collapse of whole infected plants [46]. Therefore, the search for novel antifungal agents has been a constant hot research topic in pesticide development, especially because long-term usage of the same antifungal agent often leads to an increase in the resistance of phytopathogenic fungi [47].

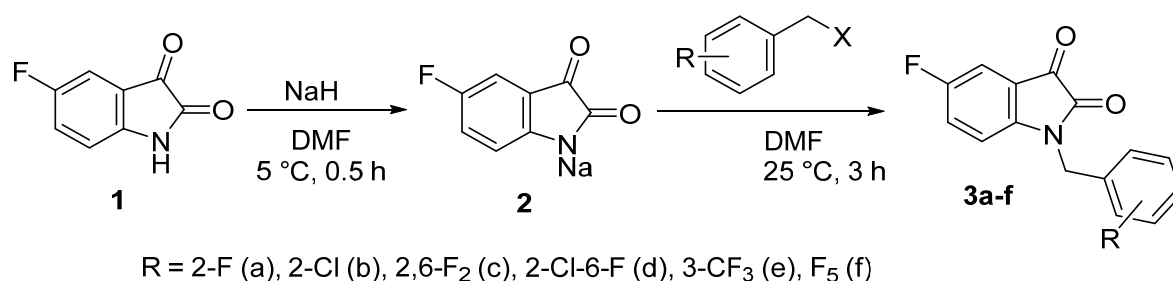
In this work, we present novel fluorinated 1-benzylisatins and water-soluble hydrazones as a platform for the search for potential antitumor and antiphytopathogenic compounds.

2. Results and Discussion

2.1. Chemistry

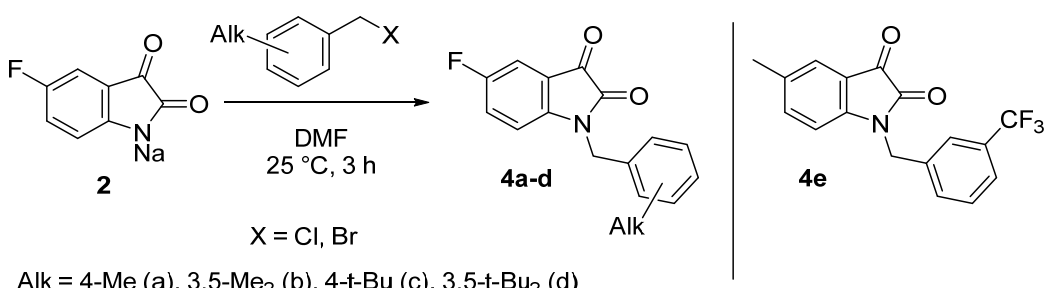
2.1.1. Synthesis of Diversely Fluorinated 1-benzylisatins

Fluoro-substituted derivatives **3a–f** were synthesized by alkylation of 5-fluoro-isatin sodium salt **2** with halogen-containing benzyl halides (Scheme 1). Isatins **3a,c,e,f** contained only F-substituents but in different substitution patterns. In addition, we have prepared a mono-chloro isatin **3b** and a mixed 2-chloro-6-fluoro derivative **3d** in order to assess the contribution of the fluorine atom in the pendant benzene ring to the biological activity.

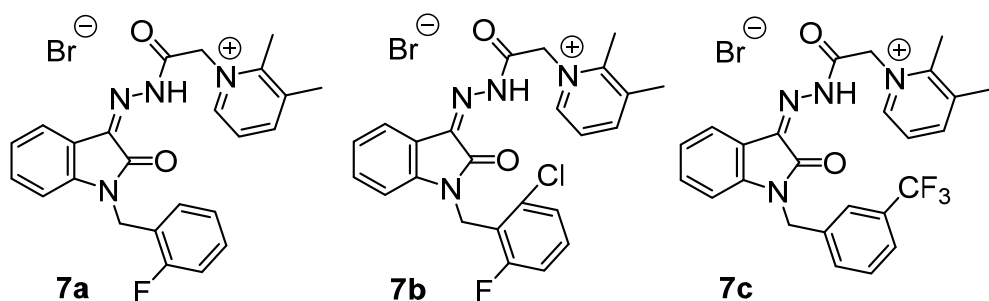
**Scheme 1.** Two-step one-pot synthesis of polyfluorinated 1-benzylisatins.

The halogenated isatins **3a–f** were isolated in high yields in their pure form immediately after the workup of the reaction mixtures. Their structure and purity have been unequivocally proven by IR and NMR spectroscopy and elemental analysis data (Figures S3–S61, Supplementary Materials).

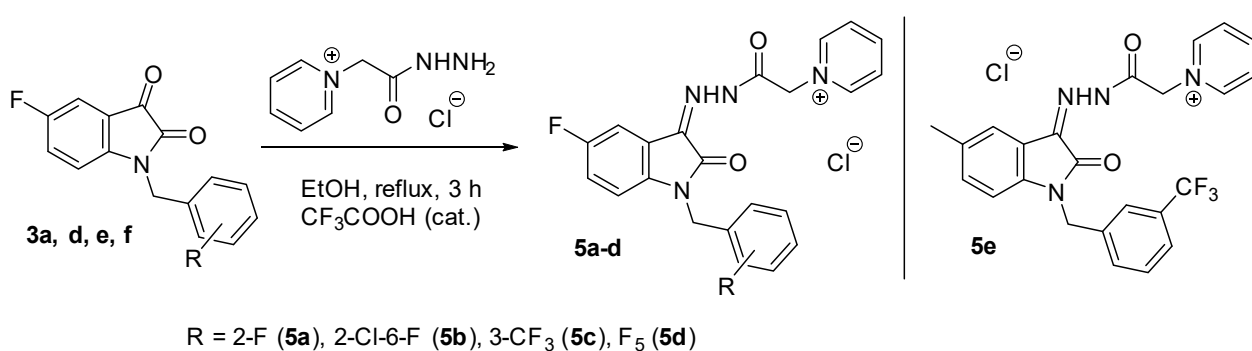
To further assess the effect of the position of the fluorine atom and the electronic structure of substituents in the benzyl fragment on the level of antitumor activity, a small series of derivatives **4a–e** was obtained by analogy (Scheme 2). In contrast to the reactions described in Scheme 1, the alkylation of sodium salt **2** by less electrophilic benzylic halides requires heating in order to achieve higher yields of the target compounds.

**Scheme 2.** Synthesis of 5-fluorinated 1-alkylbenzylisatins.

In continuation of our research on the synthesis and biological activity of water-soluble isatin-3-acylhydrazones (for example, see [23–26]), we also synthesized several new pyridinium acylhydrazones (**5a–e**) and previously published more lipophilic analogs (**7a–c**) [26] (Figure 3) containing fluorine atoms in various molecular fragments (Scheme 3).

**Figure 3.** Previously published [26] fluorinated dimethylpyridinium isatin hydrazones.

Compounds **5a–e** and **7a–c** were isolated in high yields (72–90%) after spontaneous cooling of the reaction mixture. They are yellow powders that are soluble in water, aqueous DMSO, and DMF but insoluble in non-polar solvents such as ethanol, chloroform, etc.



Scheme 3. Synthesis of fluorine-containing pyridinium isatin hydrazones.

2.1.2. X-ray Study

According to X-ray data (Figure 4A,B, Table S1, Figures S1 and S2), compounds **3f** and **4c** crystallize in different orthorhombic space groups: compound **3f** crystallizes in the non-centrosymmetric racemic space group *Pna2*₁, and compound **4c** crystallizes in the centrosymmetric space group *Pbca*.

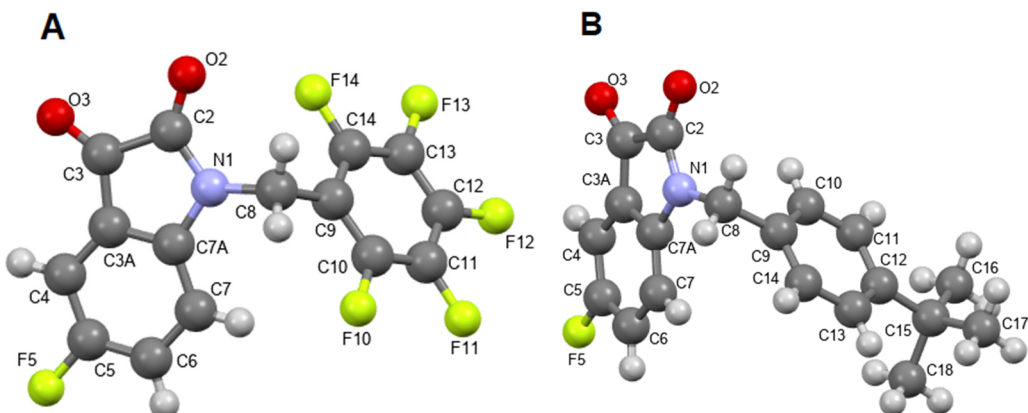


Figure 4. X-ray geometry of fluorinated isatins **3f** (A) and **4c** (B) in the crystals. Ellipsoids are shown with a 50% probability.

The conformations of the molecules in the crystals are similar: the isatin fragments are planar, and the nitrogen atom N1 has planar trigonal coordination, as is typical for amides. The benzyl substituents at the nitrogen atom are positioned non-symmetrically along the N–C8 and C8–C9 bonds. Torsion angles C2–N1–C8–C9 and N1–C8–C9–C10(C14) in the molecule are **3f** $-110.3(5)^\circ$ and $-114.0(5)^\circ$, while in the molecule **4c**, they are $-109.5(2)^\circ$ and $-132.4(2)^\circ$, respectively. This arrangement places one of the hydrogen atoms at the C8 atom in a nearly eclipsed conformation with the plane of the pendant benzene ring. In this case, the main geometric parameters (bond lengths and bond angles) in molecules **3f** and **4c** are usual.

Analysis of short contacts in crystals shows multiple C–H...F intermolecular contacts, contributing to crystal packing for these compounds. Such contacts can be considered non-conventional H-bonds [48]. This observation suggests that the C–F bonds may participate in similar supramolecular interactions with their biological targets.

Thus, using simple and efficient synthetic procedures, we obtained various fluorine-containing oxindole derivatives, which can be divided into two main groups: isatins and isatin-3-hydrzones. In the next step, we proceeded to study their biological activity.

2.2. Biological Studies

In this work, we approached it from two main angles: for substituted isatins, we evaluated the potential of using these substances as antitumor drugs, and for pyridinium hydrazones, we assessed their prospects as antiphytopathogenic agents (Figure 5).

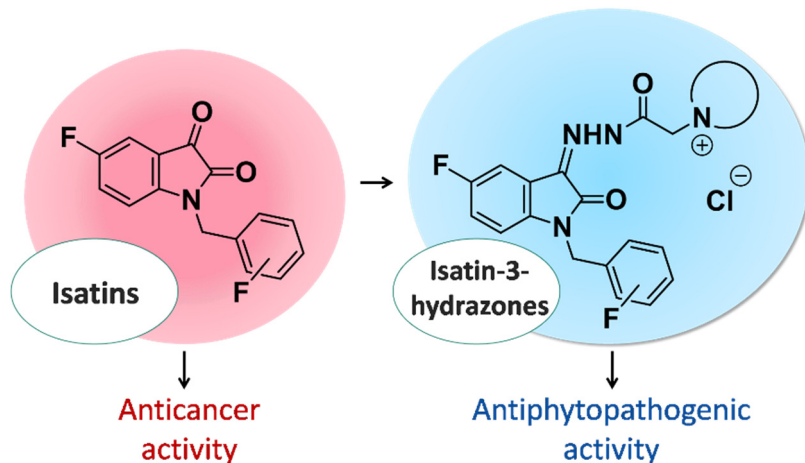


Figure 5. Different biological activity profiles of fluorinated isatin derivatives.

2.2.1. Anticancer Activity

The antitumor potential of the isatin derivatives synthesized in this work (**3a–6c**) and previously obtained (**8a–8d**) [26] (Figure 6) was primarily assessed by the ability of the compounds to reduce the survival rate of M-HeLa and HuTu 80 tumor-derived cells relative to that for normal (Chang liver) cells. Further, in order to understand the possible mechanisms of the cytotoxic action of the most promising substances, the ability to induce apoptosis and reactive oxygen species (ROS) production was determined. Additionally, the anticoagulant and antiaggregation properties were studied.

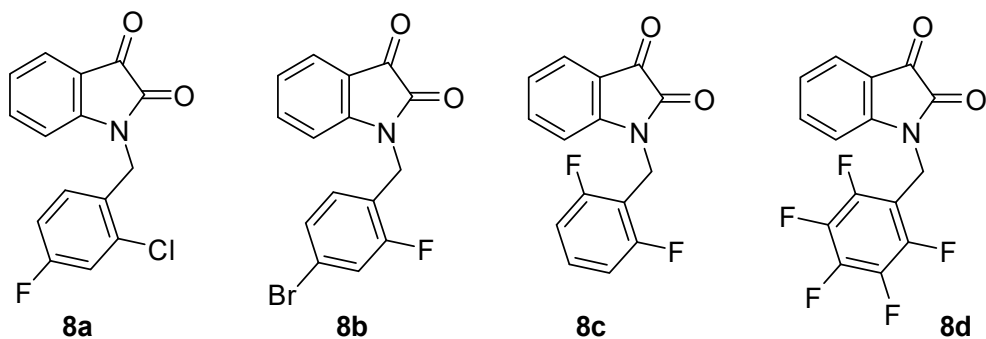


Figure 6. Previously published fluoroisatins are under investigation.

Cytotoxicity of Test Compounds

The toxic effects of all test compounds on cancer and normal cells were evaluated. The cytotoxicity of synthesized isatins was compared with the currently used antitumor drug 5-fluorouracil (5-FU) [49].

All test compounds exhibit moderate activity against the cancer lines used in the experiments (Table 1, Figure S62). Compounds **3a**, **3b**, and **3d**, containing an ortho-substituted benzyl fragment with fluorine (**3a**), chlorine (**3b**), or both (**3d**) atoms, have the highest activity against all tumor cell lines. It should be noted that for substance **3b**, the cytotoxicity is 2.0 times higher than the activity of the reference drug 5-FU. Moreover, compounds **3a**, **3b**, and **3d** had low cytotoxicity against the healthy cell line WI38.

Table 1. Cytotoxic activity (IC_{50}) and selectivity (SI) of synthesized isatins *.

Compounds	IC ₅₀ (μM)			
	^a M-HeLa	^b HuTu 80	^c Chang Liver	^d WI38
3a	74.6 ± 5.9	25.2 ± 1.9 (SI~2.5) WI38	53.0 ± 4.2	62.0 ± 2.0
3b	32.1 ± 2.5 (SI~1.8) WI38	38.3 ± 3.0 (SI~1.5) WI38	71.5 ± 5.6	58.1 ± 6.6
3c	65.7 ± 5.9	41.2 ± 2.7	95.5 ± 8.0	nd
3d	53.8 ± 4.3 (SI~1.5) WI38	31.0 ± 2.4 (SI~2.5) WI38	>100	78.3 ± 8.0
3f	100 ± 7.4	92.0 ± 6.4	>100	nd
4a	44.7 ± 3.3	44.0 ± 2.9	80.0 ± 5.8	nd
4b	58.8 ± 4.4	50.0 ± 3.8	63.2 ± 5.5	nd
4c	>100	43.0 ± 3.0	92.1 ± 7.4	nd
4d	58.4 ± 4.1	33.3 ± 2.3	39.4 ± 2.8	nd
4e	94.0 ± 7.5	53.2 ± 3.9	>100	nd
6a	98.0 ± 6.8	100 ± 8.4	76.1 ± 5.3	nd
6b	44.4 ± 3.2	37.6 ± 2.6	76.0 ± 5.4	nd
6c	83.0 ± 5.7	59.4 ± 4.2	>100	nd
8a	50.0 ± 3.7	64.0 ± 4.5	>100	nd
8b	40.0 ± 2.8	59.4 ± 4.2	100 ± 8.4	nd
8c	98.8 ± 6.9	50.3 ± 3.6	79.0 ± 5.5	nd
8d	>100	54.1 ± 3.9	>100	nd
5-FU	62.0 ± 4.9	65.2 ± 5.6	19.0 ± 1.7	62.0 ± 4.2

* The incubation time was 24 h; ^a M-HeLa—human cervical epithelioid carcinoma cell lines; ^b HuTu-80—human duodenal adenocarcinoma cell lines; ^c Chang liver—human hepatocyte-like cells; ^d WI38 is a diploid human cell strain composed of fibroblasts derived from healthy lung tissue; 5-FU—5-fluorouracil; nd—no experimental data. Experiments were carried out in triplicate.

The selectivity of compounds for cancer cells is an important criterion for evaluating a potential drug. The calculated selectivity values (SI) for the most active compounds were 1.8 for M-HeLa for **3b**, 1.5 for **3d**, and HuTu-80 for **3a**—2.5, **3b**—1.5, and **3d**—2.5, for 5-FU ≤ 1. The selectivity values (SI) indicated in the table prove that the halogenated isatins exhibit better selectivity than the reference drug 5-FU.

Apoptosis

It is well known that tumor cells are able to avoid apoptosis, which leads to uncontrolled, abnormal proliferation and rapid tumor growth. Substances capable of inducing apoptotic death in tumor cells are promising agents in the fight against cancer [50]. Flow cytometry (Guava easyCyté, Merck, Rahway, NJ, USA) showed that the most cytotoxic compounds (**3a**, **3b**, and **3d**) were able to induce apoptosis in HuTu-80 cells. Figure 7 shows the apoptotic effects induced by the selected substances at $IC_{50}/2$ and IC_{50} cytotoxicity concentrations.

It can be seen from the presented data that after 24-hour incubation of HuTu 80 cells with compounds **3a**, **3b**, and **3d**, the number of cells at both the early and late stages of apoptosis increases with concentration. Molecule **3b** exhibits the highest apoptosis-inducing activity (IC_{50} concentration of 40 μM). Moreover, in the presence of these compounds, cells exist predominantly in the stage of late apoptosis.

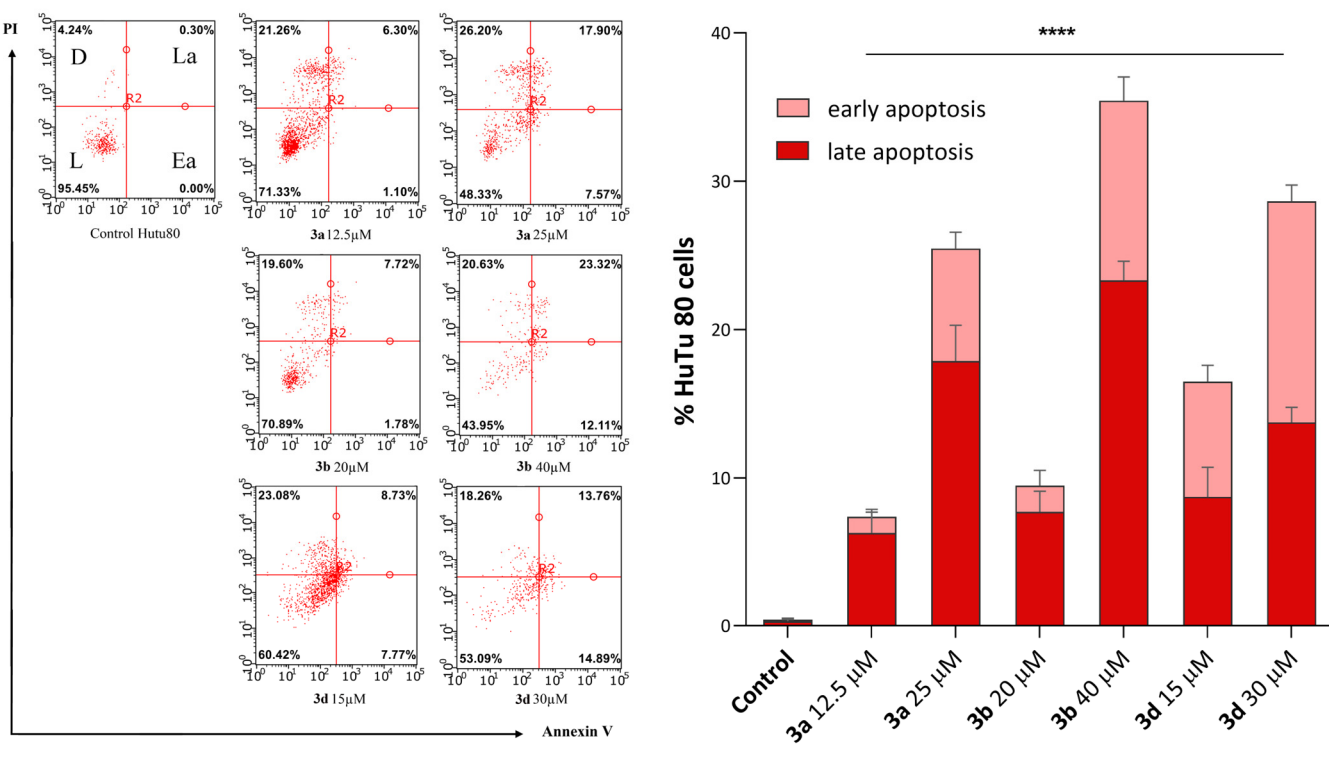


Figure 7. (a) Apoptosis induction in HuTu 80 cells incubated with compounds **3a**, **3b**, and **3d** at $IC_{50}/2$ and IC_{50} concentrations. (b) Values are presented as mean \pm standard deviation (in triplicate), L—live cells; D—dead cells; Ea—cells in early apoptosis; La—cells in late apoptosis; and PI—propidium iodide. ***— $p < 0.0001$ versus control. The statistical analysis was performed using a two-way ANOVA and the Bonferroni test.

Mitochondrial Membrane Potential

As can be seen in Figure 8, after 24-h incubation of HuTu 80 cells with the tested substances, a decrease in the mitochondrial membrane potential is observed, which becomes more pronounced at concentrations corresponding to the IC_{50} values of cytotoxicity. Compounds **3b** and **3d** showed the highest activity in this test, under the action of which the green fluorescence increased up to 55% relative to the control.

Thus, these results confirm that the mechanism of action of compounds **3a**, **3b**, and **3d** is associated with the induction of apoptosis due to the ability of substances to dissipate the mitochondrial membrane.

Reactive Oxygen Species Production

An increase in the production of reactive oxygen species (ROS) by the halogenated isatins is another characteristic feature of the development of apoptosis along the mitochondrial pathway. Mitochondria are both a potential source and a target of ROS. ROS are known to lead to disruption of mitochondrial functions and, consequently, irreversible cell damage [51].

We have evaluated the effect of compounds **3a**, **3b**, and **3d** in HuTu 80 cells on the induction of ROS production using a flow cytometry assay and the CellROX® Deep Red flow cytometry kit. The results are presented in Figure 9.

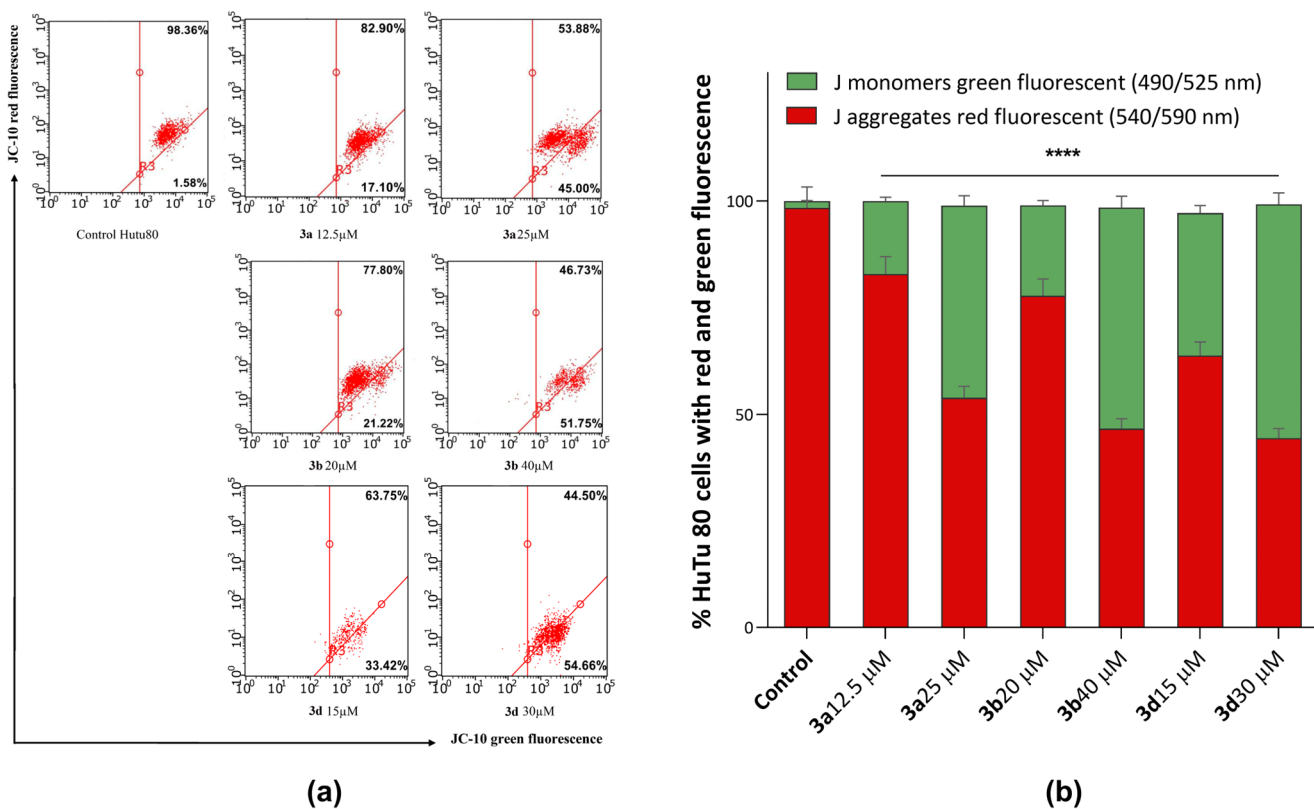


Figure 8. (a) Effects of compounds **3a**, **3b**, and **3d** on mitochondrial membrane potential. (b) Quantitative distribution of HuTu 80 cells in % with red aggregates and green monomers. ***— $p < 0.0001$ versus control. The statistical analysis was performed using a two-way ANOVA and the Bonferroni test.

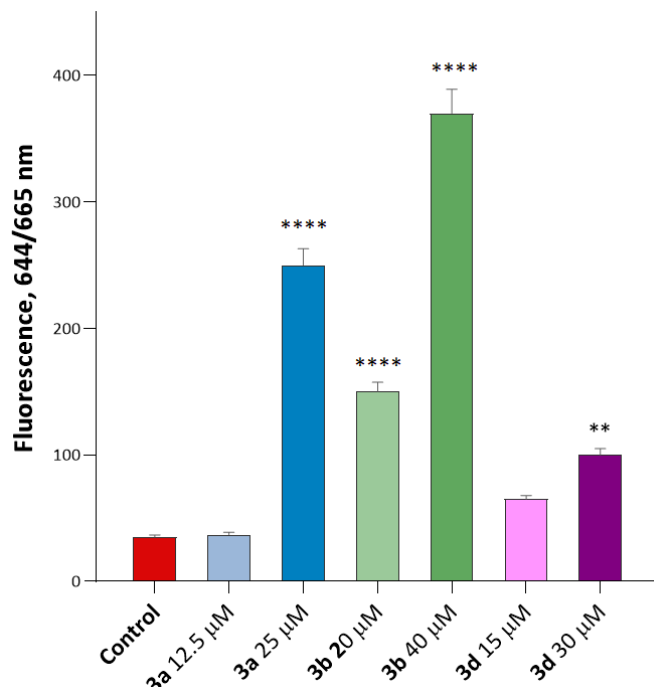


Figure 9. Induction of ROS production by compounds **3a**, **3b**, and **3d**. The data show a significant dose-dependent increase in CellROX® Deep Red fluorescence intensity for compounds **3a** and **3b**. Interestingly, compound **3a** showed only a small (1.1-fold) increase in ROS production at 12.5 μ M.

(below its IC₅₀), but the ROS production increased to 7.1 times relative to the control at 25 μ M. This indicates a significant dose-dependent increase in ROS production in the presence of this substance. Other substituted isatins **3b** and **3d** led to increased ROS production relative to the control. **— $p < 0.01$ and ***— $p < 0.0001$ versus control. The statistical analysis was performed using a one-way ANOVA and the Dunnett test.

Anticoagulant and Antiaggregation Activity Studies

In this work, for the three most promising compounds (**3a**, **3b**, and **3d**), anticoagulant and antiaggregation properties were studied (Table 2).

Table 2. Anticoagulant and antiaggregation activity of compounds **3a**, **3b**, and **3d**.

Compounds	Latent Period, % of Control	Maximum Amplitude (MA), % of Control	Aggregation Rate, % of Control	Time to MA, % of Control	APTT \$, % of Control
3a	+12.3 (11.7–14.5) *,†,‡	−11.8 (9.4–14.3) *,†	−12.7 (10.8–15.7) *,†	−8.7 (7.6–10.8) *,†,‡	+11.2 (9.5–13.7) *
3b	+10.3 (7.3–11.8) *,†,‡	−15.3 (13.9–17.2) *,†	−16.8 (14.6–19.1) *,†,‡	+9.3 (8.7–11.4) *,†	+8.3 (6.4–9.1) *
3d	+2.4 (1.3–2.7) †,‡	−8.2 (6.1–10.5) *,†,‡	−15.7 (11.9–17.6) *,†	+17.5 (16.4–18.7) *,†	+6.2 (4.7–10.3) *
Acetylsalicylic acid	−2.1 (1.1–2.6) †	−13.7 (10.8–16.4) *,†	−10.5 (7.6–12.3) *,†	+10.5 (8.7–13.4) *,†	—
Heparin sodium	—	—	—	—	+20.3 (19.7–21.4) *

* $p \leq 0.05$; # $p \leq 0.05$; † $p \leq 0.05$; \$ APTT—activated partial thromboplastin time.

Among the studied classes of compounds, derivatives **3a** and **3b** showed antiaggregation activity at the level of acetylsalicylic acid, reducing the maximum platelet aggregation by 12% on average. At the same time, compounds **3a** and **3b**, in contrast to acetylsalicylic acid, lengthen the lag-period by more than 10% relative to the control. From the point of view of anticoagulant properties, all compounds, including **3d**, showed a different level of influence on the plasma component of the hemostasis system, which manifested itself in a change in only the indicator of the internal blood coagulation pathway—activated partial thromboplastin time (APTT). Thus, fluorine-containing isatins and corresponding water-soluble acylhydrazones have high potential as scaffolds for the development of effective anticoagulant and antiaggregation agents.

The isatin derivatives synthesized in this work have the potential to be used as a basis for the design of antitumor agents with a known mechanism of action. The most cytotoxic compounds are capable of inducing the production and accumulation of reactive oxygen species by disrupting the normal functioning of mitochondria and dissipating the mitochondrial membrane. These pathological processes, provoked by the action of substances, lead to the launch of a cascade of cell death along the internal pathway of apoptosis, which is directly associated with mitochondria.

2.2.2. Evaluation of Antiphytopathogenic Activity of Water-Soluble Hydrazones Antibacterial Activity

We examined the synthesized isatin derivatives for their antibacterial effects against the above-tested organisms. Along with the solutions of **5a–e** and **7a–c**, test compounds were sodium hypochlorite (1000 μ g/mL), chlorohexidin (500 μ g/mL), and norfloxacin (500 μ g/mL), a synthetic fluoroquinolone with broad-spectrum antibacterial activity against most bacteria [52]. The in vitro bactericidal activity of the target compounds **5a–e** and **7a–c** against five representative phytopathogens is summarized in Table S2.

The results showed bactericidal activity distinct from zero against *M. luteus* B-109, *P. atrosepticum* 1043, *P. carotovorum* subsp. *carotovorum* MI, *Ps. fluorescens* EL-2.1, and *X. campestris* B-610 for all the compounds tested.

Compounds **5a**, **5b**, **5d**, and **7a** showed moderate bactericidal activity (Table S2).

Even though four compounds (**5a**, **5b**, **5d**, and **7a**) demonstrated non-zero bactericidal action, there were worse results in **7a** when affecting *M. luteus*, and in **5b**, **5d** vs. *X. campestris*, the inhibition zone width was less than 3 mm. The higher antibacterial potential

was revealed for hydrazone **7a**, with a broader spectrum against *P. carotovorum* subsp. *carotovorum* MI, *Ps. fluorescens* EL-2.1, and *X. campestris* B-610, as well as a wider inhibition zone (5–6 mm).

Compounds **5c**, **5e**, **7b**, and **7c** could be arranged into a group exhibiting a more potent ability to combat bacterial pathogens under study (Table S3, Figure 10).

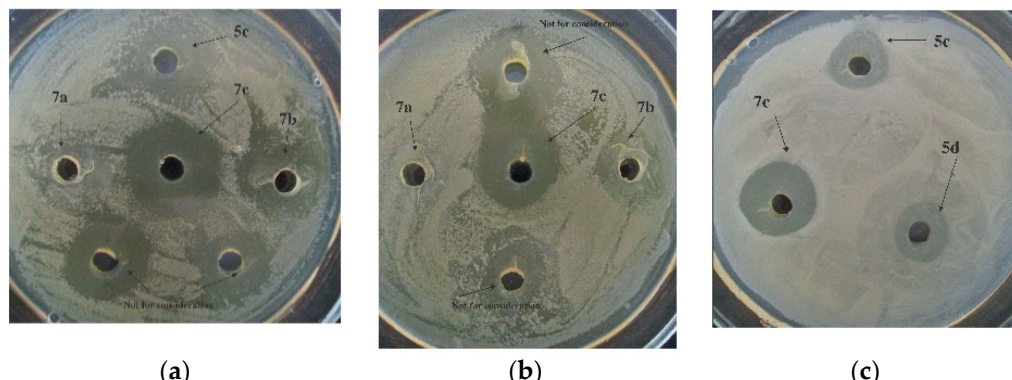


Figure 10. Bactericidal action of compounds **5c**, **5d**, and **7a–c** against *X. campestris* B-610 (a), *Pseudomonas fluorescens* EL-2.1 (b), and *P. carotovorum* subsp. *carotovorum* MI (c) at C = 1000 µg/mL.

The structural peculiarity of the compounds **7a**, **7b**, and **7c** is that they are 2,3-dimethylpyridin-1-ium salts, whereas all other hydrazones (**5a**, **5b**, **5c**, **5d**, and **5e**) are pyridin-1-ium salts. However, the substances **5c**, **5e**, and **7b**, with distinctly structured pyridinium fragments, displayed virtually the same bactericidal effect assessed by the inhibition zone range of 4 to 7 mm, dependent on the test system used (Table S3).

Greater antibacterial activity by the given hydrazone seems to be connected to the presence of the trifluoromethyl group on the phenyl ring in the side-chain substituent. Trifluoromethylated compounds are of utmost interest due to their unique properties, including their in vitro antifungal activity [53]. However, a few previous works reported that the complicated structured trifluoro derivatives of indole displayed minimal antifungal activity against *Fusarium*, with an inhibition rate of about 73% at an as high concentration as 500 mcg/mL [54]. In our work, it was compound **7c** containing a 3-trifluoromethylbenzyl substituent at the one position of a 2-oxoindolin moiety that showed the best-in-experiment bactericidal activity. Other hydrazones from this group, **5c**, **5e**, and **7b**, displayed a slightly diminished bactericidal effect and formed a 5-mm to 7-mm zone of the pathogens' growth inhibition (Table S3).

Taking into account the data on the values of the inhibition zone width (mm), it is conditionally possible to arrange the studied 2 mM solutions of compounds **5a–e**, **7a–c** in descending order of activity as follows: **7c** (6–9 mm) > **5e** (4–7 mm) ≈ **5c** (4–7 mm) ≈ **7b** (4–7 mm) > **5a** (3–6 mm) > **7a** (2–6 mm) > **5b** (2,5–4 mm) > **5d** (2–4 mm). Thus, with respect to the phytopathogens used, the most profound activity was shown by hydrazone **7c**.

Antifungal Activity

In this study, a series of fluorine-containing pyridinium isatin hydrazones (**5a–e** and **7a–c**) was prepared, and their antifungal activities were evaluated. Along with the solutions of hydrazones, the test compounds were fludioxonil and N-cetylpyridinium chloride. These commercial, widely used fungicides capable of inhibiting the pathogenic fungi mycelium propagation served for the purpose of comparison in the course of the fungicidal effect assays. Fludioxonil is one of the most potent fungicides against the diseases of agricultural crops caused by the representatives of both *Fusarium* spp. and *Phytophthora* spp. [55]. Under laboratory conditions, the assessment of the phytopathogenic fungi's resistance to fludioxonil is conducted at concentrations ranging from 0.1 to 10 µg/mL [56]. N-cetylpyridinium chloride (CPC) is a quaternary ammonium compound with broad-spectrum antimicrobial activity [57] used in topical formulations with antifungal activity [58,59].

The in vitro antifungal activity of target compounds **5a–e** and **7a–c** against the fungal pathogen *F. oxysporum* is summarized in Table S4.

Within the entire experiment with the phytopathogen *F. oxysporum*, the highest fungicidal activity estimated through the EC₅₀ indices ($\mu\text{g}/\text{mL}$) was displayed by the studied compounds **5e** (0.60) and **7a** (7.25). Antifungal activity of the rest of the hydrazones tested was also considerable, with the EC₅₀ value not exceeding 21 $\mu\text{g}/\text{mL}$ for **7b**. The methyl group at the C5 position of the oxindole moiety, in combination with the trifluoromethyl group on the benzyl ring (**5e**) of the 1-benzylisatin hydrazones, as well as the fluorine atom at the C2 position on this benzyl ring (**7a**), had a significant effect on the pyridinium isatin hydrazones antifungal activity against *F. oxysporum* (Figure 11).

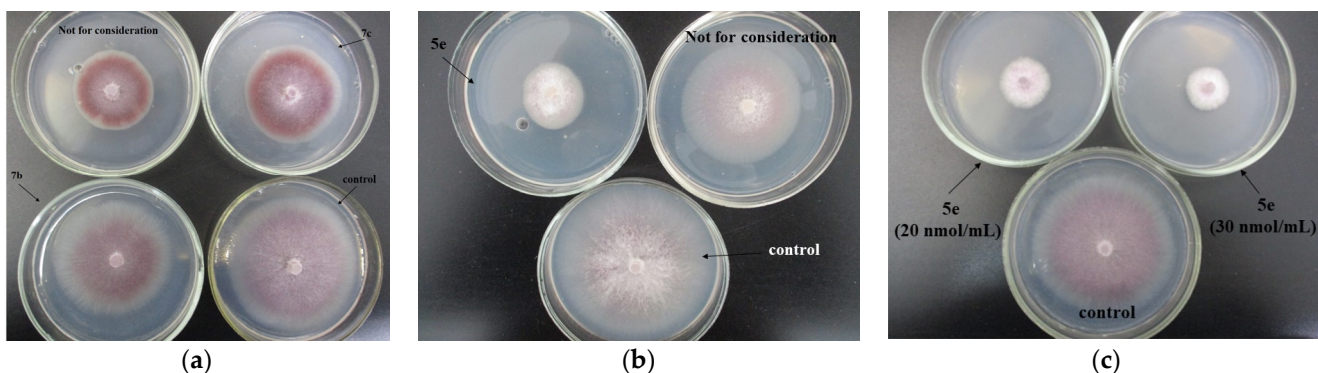


Figure 11. Growth of *Fusarium oxysporum* IBPPM 543 on agar media fortified with the compounds **7c** and **7b** (C 20 nmol/mL (a); **5e** (C 3 nmol/mL) (b); **5e** (C 20 and 30 nmol/mL) (c)).

Compound **5e** had the most significant antifungal activity against *F. oxysporum* (IC₅₀ = 0.60 $\mu\text{g}/\text{mL}$).

The in vitro antifungal activity of target compounds **5a–e** and **7a–c** against the fungal pathogen *P. cactorum* is summarized in Table S5.

Within the entire experiment with the phytopathogen *P. cactorum*, the highest fungicidal activity assessed through the EC₅₀ parameter ($\mu\text{g}/\text{mL}$) was displayed by the studied compounds **5a** (15.12), **5c** (15.40), and **5b** (18.19). Antifungal activity of the rest of the tested hydrazones was also considerable, with the EC₅₀ value not exceeding 28 $\mu\text{g}/\text{mL}$ for **7b**. The fluorine atom (**5a**, **5b**, and **5c**) at the C5 position of the isatin skeleton in the pyridinium isatin hydrazones, in combination with the strong electron-withdrawing units: the trifluoromethyl group (-CF₃) (**5c**), the fluorine atom at the C2 position (**5a**), or the 2-Cl-6-F (**5b**) substituent on the benzyl ring of the 1-benzylisatin hydrazones, had a significant effect on the improvement of the antimicrobial activity against *P. cactorum*. Compounds **5a** and **5c** exhibited essentially the same antifungal activity, equal to 15 $\mu\text{g}/\text{mL}$.

All of the fluorine-containing compounds (**5a–e** and **7a–c**) showed an antagonistic effect against the oomycete *P. cactorum*. This effect is somewhat superior to that of N-cetylpyridinium chloride by 1.3 (**5e**, **7b**) to 2.3 (**5a**, **5c**) times and of fludioxonil by 1.1 (**5e**, **7b**) to 2.0 (**5a**) times in 5 days of *Phytophthora* growth. At the same culture age as ascomycete *F. oxysporum*, all of the studied fluorine-containing compounds outperformed the reference fungicides in the antifungal effect of this test system. Fludioxonil was less efficient than hydrazones in inhibiting *Fusarium* growth. Inhibition by hydrazone ranged from 139 times greater than **5e** down to 4.1 times greater than **7b**. N-cetylpyridinium chloride showed weaker fungicidal action vs. *F. oxysporum*, as compared to **5a–e** and **7a–c**, by 235 times more than **5e** and down to 7.0 times more than **7b**.

When comparing the fungicidal activity of hydrazones in the *F. oxysporum* test system and their antagonistic action with respect to *P. cactorum*, one can recognize that, without exceptions, all compounds under study show the greater ability to inhibit the mycelial propagation of *F. oxysporum* (Table 3).

Table 3. Comparative fungicidal activity of hydrazones **5a–e** and **7a–c** against *Fusarium oxysporum* IBPPM 543 and *Phytophthora cactorum* VKM F-985.

Compound	EC ₅₀ , µg/mL * at Day 5	
	<i>F. oxysporum</i>	<i>P. cactorum</i>
5a	13.84	15.12
5b	14.84	18.19
5c	14.92	15.40
5d	17.35	24.74
5e	0.60	27.43
7a	7.25	22.87
7b	20.24	27.51
7c	13.90	19.98
Fludioxonil	83.33	29.51
N-cetylpyridinium chloride	141.1	34.79

* The average values are given; the standard deviation did not exceed 0.03 from the given value.

The inhibiting action of fluorine-containing hydrazones **5a–e**, **7a–c** judged through the EC₅₀ criterion occurred to be stronger with respect to *Fusarium* mycelial development, by 46 times more than **5e**, down to 1.1 times more than **5c**, in comparison to the same compounds' impact on *Phytophthora*. In contrast, the reference fungicides exhibited the opposite tendency for the fungal test system used. Fludioxonil and N-cetylpyridinium chloride showed a much greater effect of *P. cactorum* growth inhibition compared to *F. oxysporum* (2.8 and 4.1 times, respectively, for the two fungicides in Table 3). The behavior of the fluorine-free compounds synthesized and examined for antiphytopathogenic activity by us earlier [25] was in line with the latter tendency, i.e., they were similar to the reference fungicides. The results could testify to a promising synthetic strategy potentially resulting in the fluorine-containing hydrazones being uncommonly efficient vs. *Fusarium oxysporum* in comparison with known fungicides.

3. Materials and Methods

3.1. Chemistry

IR spectra were recorded on the IR Fourier spectrometer Tensor 37 (Bruker Optik GmbH, Ettlingen, Germany) in the 400–3600 cm⁻¹ range in KBr. The ¹H-, ¹⁹F-, and ¹³C-NMR spectra were recorded on a Bruker AVANCE 400 spectrometer (Bruker BioSpin, Rheinstetten, Germany) operating at 400 MHz (for ¹H NMR), 377 MHz (for ¹⁹F NMR) and 101 MHz (for ¹³C NMR), Brucker spectrometers AVANCEIII-500 (Bruker BioSpin, Rheinstetten, Germany) operating at 500 MHz (for ¹H NMR) and 126 MHz (for ¹³C MMR), and Bruker Avance 600 spectrometer (Bruker BioSpin, Rheinstetten, Germany) operating at 600 MHz (for ¹H NMR) and 151 MHz (for ¹³C NMR). Chemical shifts were measured in δ (ppm) with reference to the solvent (δ = 7.27 ppm and 77.00 ppm for CDCl₃, δ = 2.50 ppm and 39.50 ppm for DMSO-d₆, for ¹H and ¹³C NMR, respectively). Elemental analysis was performed on a CHNS-O Elemental Analyser EuroEA3028-HT-OM (EuroVector S.p.A., Milan, Italy). The melting points were determined on the Stuart SMP10 apparatus (Stuart, Birmingham, UK).

X-ray crystallography data. Data for **3f** and **4c** were collected on a Bruker D8 QUEST with a PHOTON II CCD diffractometer (Bruker AXS, Karlsruhe, Germany), using graphite monochromated MoKα (λ = 0.71073 Å) radiation and ω-scan rotation. Dataset collection images were indexed, integrated, and scaled using the APEX3 [60] dataset reduction package and corrected for absorption using SADABS [61]. The structure was solved by direct methods and refined using the SHELX program [62]. All non-hydrogen atoms were refined anisotropically. H atoms were calculated on idealized positions and refined as riding

atoms. Crystal Data and Refinement Details are presented in Table S1 (see Supplementary Materials). The X-ray analysis was performed on the equipment of the Spectral-Analytical Center of FRC Kazan Scientific Center of RAS.

CCDC 2268269 and 2268273 (**3f** and **4c**) contain the supplementary crystallographic data for this paper. These data can be obtained free of charge via www.ccdc.cam.ac.uk/conts/retrieving.html (accessed on 16 September 2023) or from the Cambridge Crystallographic Data Centre, 12 Union Road, Cambridge CB2 1EZ, UK; fax: (+44) 1223-336-033; or deposit@ccdc.cam.ac.uk.

Synthesis of fluorine-containing indolin-2,3-diones (isatins) **3a–f** and **4a–e** (general method). A magnetically stirred solution of 5-substituted isatin **1** (10 mmol) in dry DMF (20 mL) and NaH (10 mmol, 60% suspension in mineral oil) was added in portions for 30 min at 5 °C (ice-water external bath). During the addition of sodium hydride, the reaction mixture turns purple. After 30 min, the corresponding benzyl halide (10 mmol) was added dropwise, followed by additional stirring at r.t. (3 h for **3a–f** and 6 h for **4a–e**). Then, a solution was poured into an ice/water mixture (*w/w* 100 g/200 g), and the precipitate that formed was filtered off, washed consecutively with cold water (50 mL), light petroleum (40 mL), and dried in vacuo (12 Torr). For better precipitation of the target product in the case of alkylbenzyl isatins, sodium chloride (10 g) was added to the mixture of ice and water.

5-Fluoro-1-(2-fluorobenzyl)indoline-2,3-dione (3a). Orange powder. Yield 95%, m.p. = 120–121 °C. IR spectrum, ν , cm⁻¹: 1333 (C–F), 1621 (C=C), 1732 (C=O), 3066 (CH). ¹H NMR (600 MHz, CDCl₃) δ 7.37–7.28 (m, 3H, Ph), 7.26–7.21 (m, 1H, Ar), 7.15–7.08 (m, 2H, Ar), 6.88 (dd, *J* = 8.6 Hz, *J* = 3.6 Hz, 1H, Ar), 4.97 (s, 2H, CH₂). ¹³C NMR (151 MHz, CDCl₃) δ 182.4, 160.8 (d, *J* = 176.9 Hz, C–F), 159.2 (d, *J* = 176.5 Hz, C–F), 158.1, 146.5, 130.3 (d, *J* = 8.1 Hz, C–F, CH), 130.0 (d, *J* = 1.8 Hz, C–F, CH), 124.9 (d, *J* = 2.4 Hz, C–F, CH), 124.8 (d, *J* = 24.2 Hz, C–F, CH), 121.4 (d, *J* = 14.3 Hz, C–F), 118.3 (d, *J* = 6.9 Hz, C–F), 115.8 (d, *J* = 21.6 Hz, C–F, CH), 112.4 (d, *J* = 24.3 Hz, C–F, CH), 111.9 (d, *J* = 3.1 Hz, C–F, CH), 37.4 (d, *J* = 4.0 Hz, C–F, CH₂). ¹⁹F NMR (600 MHz, DMSO-*d*₆) δ –119.9, –119.5. Found: C, 65.87; H, 3.34; F, 13.83; N, 5.11. Anal. calcd (%) for C₁₅H₉F₂NO₂: C, 65.94; H, 3.32; F, 13.91; N, 5.13.

1-(2-Chlorobenzyl)-5-fluoroindoline-2,3-dione (3b). Light orange powder. Yield 76%, m.p. = 167–168 °C. IR spectrum, ν , cm⁻¹: 746 (CCl), 1344 (C–F), 1620 (C=C), 1733 (C=O), 3061 (CH). ¹H NMR (500 MHz, CDCl₃) δ 7.43 (d, 1H, *J* = 7.4 Hz, Ar), 7.34 (dd, *J* = 6.5 Hz, *J* = 2.7 Hz, 1H, Ar), 7.29–7.19 (m, 4H, Ar), 6.74 (dd, *J* = 8.6 Hz, *J* = 3.5 Hz, 1H, Ar), 5.06 (s, 2H, CH₂). ¹³C NMR (126 MHz, DMSO-*d*₆) δ 182.1 (d, *J* = 1.6 Hz, C–F), 158.6 (d, *J* = 241.2 Hz, C–F), 158.5, 146.4, 132.2 (CH), 131.8, 129.4 (d, *J* = 22.8 Hz, C–F, CH), 128.3 (CH), 127.4 (CH), 123.9, 123.7, 118.9 (d, *J* = 7.0 Hz, C–F), 112.2 (d, *J* = 7.6 Hz, C–F, CH), 111.5 (d, *J* = 24.4 Hz, C–F, CH), 41.2 (CH₂). ¹⁹F NMR (600 MHz, DMSO-*d*₆) δ –119.8. Found: C, 62.21; H, 3.15; Cl, 12.19; F, 6.46; N, 4.78. Anal. calcd (%) for C₁₅H₉ClFNO₂: C, 62.19; H, 3.13; Cl, 12.24; F, 6.56; N, 4.84.

1-(2,6-Difluorobenzyl)-5-fluoroindoline-2,3-dione (3c). Red powder. Yield 85%, m.p. 131–132 °C. IR spectrum, ν , cm⁻¹: 1327 (C–F), 1623 (C=C), 1735 (C=O), 1753 (C=O), 3057 (CH). ¹H NMR (500 MHz, CDCl₃) δ 7.34–7.28 (m, 2H, Ar), 7.24 (ddd, *J* = 8.8 Hz, *J* = 8.7 Hz, *J* = 2.7 Hz, 1H, Ar), 6.94 (dd, *J* = 8.1 Hz, *J* = 8.0 Hz, 1H, Ar), 6.88 (dd, *J* = 8.7 Hz, *J* = 3.6 Hz, 1H, Ar), 5.02 (s, 2H, CH₂). ¹³C NMR (126 MHz, CDCl₃) δ 182.3, 161.5 (dd, ¹J = 250.4 Hz, ³J = 7.3 Hz, C–F), 159.3 (d, *J* = 246.1 Hz, C–F), 157.3 (d, *J* = 0.6 Hz, C–F), 146.3 (d, *J* = 2.0 Hz), 130.7 (t, *J* = 10.4 Hz, C–F, CH), 124.7 (d, *J* = 24.2 Hz, C–F, CH), 118.4 (d, *J* = 7.0 Hz, C–F), 112.4 (dd, *J* = 24.2 Hz, *J* = 0.3 Hz, C–F, CH), 111.8 (dd, *J* = 25.1 Hz, *J* = 6.1 Hz, C–F, CH), 111.5 (dt, *J* = 9.2 Hz, *J* = 2.4 Hz, C–F, CH), 109.9 (t, *J* = 18.2 Hz, C–F), 32.3 (t, *J* = 4.0 Hz, C–F, CH₂). Found: C, 61.80; H, 2.80; F, 19.45; N, 4.77. Anal. calcd (%) for C₁₅H₈F₃NO₂: C, 61.86; H, 2.77; F, 19.57; N, 4.81.

1-(2-Chloro-6-fluorobenzyl)-5-fluoroindoline-2,3-dione (3d). Bright orange powder. Yield 90%, m.p. = 140–141 °C. IR spectrum, ν , cm⁻¹: 779 (CCl), 1330 (C–F), 1624 (C=C), 1745 (C=O), 1772 (C=O), 3070 (CH). ¹H NMR (500 MHz, CDCl₃) δ 7.32–7.27 (m, 3H, Ar), 7.20 (ddd, *J* = 8.7 Hz, *J* = 8.7 Hz, *J* = 2.7 Hz, 1H, Ar), 7.07–7.02 (m, 1H, Ar), 6.80 (dd, *J* = 8.7 Hz,

$J = 3.6$ Hz, 1H, Ar), 5.12 (d, $J = 0.8$ Hz, 2H, CH₂). ¹³C NMR (126 MHz, DMSO-*d*₆) δ 182.2 (d, $J = 0.7$ Hz, C–F), 161.4 (d, $J = 249.7$ Hz, C–F), 158.4 (d, $J = 241.6$ Hz, C–F), 157.8, 146.8, 134.3 (d, $J = 5.3$ Hz, C–F, CH), 130.9 (d, $J = 10.0$ Hz, C–F), 125.9 (d, $J = 2.9$ Hz, C–F, CH), 124.3 (d, $J = 24.2$ Hz, C–F, CH), 120.3 (d, $J = 16.4$ Hz, C–F), 118.5 (d, $J = 7.4$ Hz, C–F), 114.9 (d, $J = 22.5$ Hz, C–F, CH), 112.0 (d, $J = 6.3$ Hz, C–F, CH), 111.6 (d, $J = 24.4$ Hz, C–F, CH), 36.2 (d, $J = 3.2$ Hz, C–F, CH₂). ¹⁹F NMR (600 MHz, DMSO-*d*₆) δ –119.8, –111.0. Found: C, 58.60; H, 2.59; Cl, 11.48; F, 12.23; N, 4.54. Anal. calcd (%) for C₁₅H₈ClF₂NO₂: C, 58.56; H, 2.62; Cl, 11.52; F, 12.35; N, 4.55.

5-Fluoro-1-(3-(trifluoromethyl)benzyl)indoline-2,3-dione (3e). Orange powder. Yield 83%, m.p. = 170–171 °C. IR spectrum, ν , cm^{–1}: 1330 (C–F), 1621 (C=C), 1731 (C=O), 1745 (C=O), 3066 (CH). ¹H NMR (400 MHz, DMSO-*d*₆) δ 7.85 (s, 1H, Ar), 7.75 (d, $J = 7.7$ Hz, 1H, Ar), 7.65 (d, $J = 7.8$ Hz, 1H, Ar), 7.58 (t, $J = 7.7$ Hz, 1H, Ar), 7.49 (dd, $J = 7.2$ Hz, $J = 2.7$ Hz, 1H, Ar), 7.45 (ddd, $J = 9.3$ Hz, $J = 8.8$ Hz, $J = 2.8$ Hz, 1H, Ar), 6.98 (dd, $J = 8.6$ Hz, $J = 3.8$ Hz, 1H, Ar), 5.01 (s, 2H, CH₂). ¹³C NMR (101 MHz, DMSO-*d*₆) δ 182.2, 158.5 (d, $J = 241.3$ Hz, C–F), 158.6, 146.2, 137.0, 131.4 (CH), 129.7 (CH), 129.3 (q, $J = 31.6$ Hz, C–F), 124.3 (m, CH), 124.1 (m, CH), 123.6 (d, $J = 24.1$ Hz, C–F, CH), 118.9 (d, $J = 7.3$ Hz, C–F), 112.1 (d, $J = 7.6$ Hz, C–F, CH), 111.5 (d, $J = 22.4$ Hz, C–F, CH), 42.5 (CH₂). Found: C, 59.40; H, 2.83; F, 23.47; N, 4.30. Anal. calcd (%) for C₁₆H₉F₄NO₂: C, 59.45; H, 2.81; F, 23.51; N, 4.33.

5-Fluoro-1-((perfluorophenyl)methyl)indoline-2,3-dione (3f). Purple powder. Yield 75%, m.p. = 112–113 °C. IR spectrum, ν , cm^{–1}: 1330 (C–F), 1625 (C=C), 1749 (C=O), 3054 (CH). ¹H NMR (500 MHz, CDCl₃) δ 7.37–7.30 (m, 2H, Ar), 6.89 (dd, $J = 8.6$ Hz, $J = 3.4$ Hz, 1H, Ar), 5.04 (s, 2H, CH₂). ¹³C NMR (126 MHz, CDCl₃) δ 181.5 (d, $J = 1.8$ Hz, C–F), 159.5 (d, $J = 247.1$ Hz, C–F), 157.3, 151.9–149.3 (m, C–F), 146.8–144.3 (m, C–F), 145.6 (d, $J = 1.7$ Hz, C–F), 142.9–140.4 (m, C–F), 136.8–136.2 (m, C–F), 124.9 (d, $J = 24.3$ Hz, C–F, CH), 118.5 (d, $J = 6.9$ Hz, C–F), 112.8 (d, $J = 24.3$ Hz, C–F, CH), 111.1 (d, $J = 7.1$ Hz, C–F, CH), 32.1 (CH₂). Found: C, 52.13; H, 1.56; F, 32.93; N, 4.00. Anal. calcd (%) for C₁₅H₅F₆NO₂: C, 52.19; H, 1.46; F, 33.02; N, 4.06.

5-Fluoro-1-(4-methylbenzyl)indoline-2,3-dione (4a). Orange powder. Yield 73%, m.p. = 111–112 °C. IR spectrum, ν , cm^{–1}: 1330 (C–F), 1623 (C=C), 1730 (C=O), 1741 (C=O), 2923 (CH). ¹H NMR (500 MHz, DMSO-*d*₆) δ 7.48–7.41 (m, 2H, Ar), 7.31 (d, $J = 8.0$ Hz, 1H, Ar), 7.14 (d, $J = 7.9$ Hz, 1H, Ar), 6.95 (dd, $J = 8.6$ Hz, $J = 3.8$ Hz, 1H, Ar), 4.86 (s, 2H, CH₂), 2.27 (s, 3H, CH₃). ¹³C NMR (126 MHz, DMSO-*d*₆) δ 182.5 (d, $J = 2.0$ Hz, C–F), 158.5 (d, $J = 241.3$ Hz, C–F), 158.3, 146.5 (d, $J = 1.4$ Hz, C–F), 136.7, 132.2, 129.2 (CH), 127.3 (CH), 123.8 (d, $J = 24.2$ Hz, C–F, CH), 118.6 (d, $J = 7.3$ Hz, C–F), 112.4 (d, $J = 7.4$ Hz, C–F, CH), 111.4 (d, $J = 24.4$ Hz, C–F, CH), 42.7 (CH₂), 20.6 (CH₃). Found: C, 71.29; H, 4.43; F, 7.00; N, 5.16. Anal. calcd (%) for C₁₆H₁₂FNO₂: C, 71.37; H, 4.49; F, 7.06; N, 5.20.

1-(3,5-Dimethylbenzyl)-5-fluoroindoline-2,3-dione (4b). Light orange powder. Yield 70%, m.p. = 97–98 °C. IR spectrum, ν , cm^{–1}: 1341 (C–F), 1623 (C=C), 1741 (C=O), 2922 (CH). ¹H NMR (400 MHz, CDCl₃) δ 7.30 (dd, $J = 6.5$ Hz, $J = 2.7$ Hz, 1H, Ar), 7.20 (ddd, $J = 8.6$ Hz, $J = 8.6$ Hz, $J = 2.7$ Hz, 1H, Ar), 6.93 (s, 1H, Ar), 6.91 (s, 2H, Ar), 6.75 (dd, $J = 8.6$ Hz, $J = 3.6$ Hz, 1H, Ar), 4.84 (s, 2H, CH₂), 2.28 (s, 6H, CH₃). ¹³C NMR (101 MHz, CDCl₃) δ 182.8 (d, $J = 1.7$ Hz, C–F), 159.3 (d, $J = 246.0$ Hz, C–F), 158.1, 146.9 (d, $J = 1.7$ Hz, C–F), 138.8, 134.0, 129.9 (CH), 125.1 (CH), 124.6 (d, $J = 24.1$ Hz, C–F, CH), 118.3 (d, $J = 7.0$ Hz, C–F), 112.4 (d, $J = 15.3$ Hz, C–F, CH), 112.2 (d, $J = 0.9$ Hz, C–F, CH), 44.1 (CH₂), 21.2 (CH₃). Found: C, 72.00; H, 4.95; F, 6.60; N, 4.90. Anal. calcd (%) for C₁₇H₁₄FNO₂: C, 72.07; H, 4.98; F, 6.71; N, 4.94.

1-(4-(*tert*-Butyl)benzyl)-5-fluoroindoline-2,3-dione (4c). Orange powder. Yield 71%, m.p. = 123–124 °C. IR spectrum, ν , cm^{–1}: 1333 (C–F), 1623 (C=C), 1734 (C=O), 2959 (CH), 3063 (CH). ¹H NMR (400 MHz, CDCl₃) δ 7.36 (d, $J = 8.6$ Hz, 2H, Ar), 7.29 (dd, $J = 6.5$ Hz, $J = 2.7$ Hz, 1H, Ar), 7.25 (d, $J = 8.6$ Hz, 2H, Ar), 7.20 (ddd, $J = 8.7$ Hz, $J = 8.7$ Hz, $J = 2.7$ Hz, 1H, Ar), 6.78 (dd, $J = 8.6$ Hz, $J = 3.6$ Hz, 1H, Ar), 4.89 (s, 2H, CH₂), 1.29 (s, 9H, CH₃). ¹³C NMR (101 MHz, CDCl₃) δ 182.7 (d, $J = 1.9$ Hz, C–F), 159.3 (d, $J = 245.9$ Hz, C–F), 158.0, 151.4, 146.9 (d, $J = 1.6$ Hz, C–F), 131.1, 127.2 (CH), 126.0 (CH), 124.5 (d, $J = 24.1$ Hz, C–F, CH), 118.2 (d, $J = 7.0$ Hz, C–F), 112.4 (d, $J = 12.6$ Hz, C–F, CH), 112.2 (d, $J = 4.4$ Hz, C–F, CH),

43.8 (CH₂), 34.5, 31.2 (CH₃). Found: C, 73.21; H, 5.80; F, 6.01; N, 4.43. Anal. calcd (%) for C₁₉H₁₈FNO₂: C, 73.30; H, 5.83; F, 6.10; N, 4.50.

1-(3,5-Di-*tert*-butylbenzyl)-5-fluoroindoline-2,3-dione (4d**).** Orange powder. Yield 72%, m.p. = 136–137 °C. IR spectrum, ν , cm^{−1}: 1342 (C—F), 1622 (C=C), 1734 (C=O), 2964 (CH), 3043 (CH). ¹H NMR (400 MHz, CDCl₃) δ 7.37 (s, 1H, Ar), 7.32 (dd, *J* = 6.4 Hz, *J* = 2.5 Hz, 1H, Ar), 7.21 (ddd, *J* = 8.6 Hz, *J* = 8.6 Hz, *J* = 2.4 Hz, 1H, Ar), 7.14 (s, 2H, Ar), 6.80 (dd, *J* = 8.6 Hz, *J* = 3.5 Hz, 1H, Ar), 4.90 (s, 2H, CH₂), 1.29 (s, 18H, CH₃). ¹³C NMR (101 MHz, CDCl₃) δ 182.8 (d, *J* = 1.9 Hz, C—F), 159.3 (d, *J* = 245.9 Hz, C—F), 158.1 (d, *J* = 1.0 Hz, C—F), 151.8, 147.1 (d, *J* = 1.7 Hz, C—F), 133.4, 124.4 (d, *J* = 24.1 Hz, C—F, CH), 122.2 (CH), 121.8 (CH), 118.3 (d, *J* = 7.0 Hz, C—F), 112.3 (d, *J* = 29.4 Hz, C—F, CH), 112.2 (CH), 44.8 (CH₂), 34.8, 31.4 (CH₃). Found: C, 75.15; H, 7.10; F, 5.09; N, 3.72. Anal. calcd (%) for C₂₃H₂₆FNO₂: C, 75.18; H, 7.13; F, 5.17; N, 3.81.

5-Methyl-1-(3-(trifluoromethyl)benzyl)indoline-2,3-dione (4e**).** Orange powder. Yield 86%, m.p. = 155–156 °C. IR spectrum, ν , cm^{−1}: 1329 (C—F), 1620 (C=C), 1728 (C=O), 1742 (C=O), 2929 (CH), 3035 (CH). ¹H NMR (500 MHz, DMSO-*d*₆) δ 7.83 (s, 1H, Ar), 7.73 (d, *J* = 7.6 Hz, 1H, Ar), 7.64 (d, *J* = 7.8 Hz, 1H, Ar), 7.57 (dd, *J* = 7.7 Hz, *J* = 7.7 Hz, 1H, Ar), 7.40–7.38 (m, 2H, Ar), 6.88 (d, *J* = 8.7 Hz, 1H, Ar), 5.00 (s, 2H, CH₂), 2.26 (s, 3H, CH₃). ¹³C NMR (126 MHz, DMSO-*d*₆) δ 183.0, 158.5, 147.9, 138.1 (CH), 137.2, 132.7 (CH), 131.3 (CH), 129.6, 129.3 (q, *J* = 31.7 Hz, C—F), 124.7 (CH), 124.2 (q, *J* = 3.8 Hz, C—F, CH), 124.1 (q, *J* = 3.7 Hz, C—F, CH), 124.0 (q, *J* = 272.4 Hz, CF₃), 117.8, 110.6 (CH), 42.4 (CH₂), 20.0 (CH₃). Found: C, 63.87; H, 3.73; F, 17.80; N, 4.38. Anal. calcd (%) for C₁₇H₁₂F₃NO₂: C, 63.95; H, 3.79; F, 17.85; N, 4.39.

Synthesis of fluorine-containing isatin-3-acylhydrazones 5 (general method). To the mixture of substituted isatin (10 mmol) and 15 mL of absolute ethanol, Girard's reagent P (10 mmol) and three drops of trifluoroacetic acid were successively added. The reaction solution was heated under reflux for 3 h. After spontaneously cooling to room temperature, the precipitate formed was filtered, washed with absolute ether, and dried in a vacuum.

1-(2-(5-Fluoro-1-(2-fluorobenzyl)-2-oxoindolin-3-ylidene)hydrazinyl)-2-oxoethyl pyridin-1-iium chloride (5a**).** Yellow powder. Yield 90%, m.p. = 180–182 °C. IR spectrum, ν , cm^{−1}: 1358 (C—F), 1621 (C=C), 1686 (C=O), 3017 (CH), 3391 (NH). ¹H NMR (500 MHz, DMSO-*d*₆) δ 12.65 (s, 1H, NH), 9.23 (d, *J* = 5.2 Hz, 2H, Ar), 8.74 (t, *J* = 7.8 Hz, 1H, Ar), 8.28 (t, *J* = 6.9 Hz, 2H, Ar), 7.50 (d, *J* = 5.9 Hz, 1H, Ar), 7.42–7.30 (m, 3H, Ar), 7.25–7.16 (m, 2H, Ar), 7.12 (dd, *J* = 8.6 Hz, *J* = 3.9 Hz, 1H, Ar), 6.33 (s, 2H, CH₂), 4.93 (s, 2H, CH₂). ¹³C NMR (126 MHz, DMSO-*d*₆) δ 167.8, 160.9 (d, *J* = 246.0 Hz, C—F), 160.4, 158.8 (d, *J* = 239.6 Hz, C—F), 158.1, 146.6 (CH), 146.5 (CH), 146.2, 139.2, 130.0 (d, *J* = 7.9 Hz, C—F, CH), 129.8 (d, *J* = 3.3 Hz, C—F, CH), 127.7 (CH), 124.7 (d, *J* = 2.8 Hz, C—F, CH), 122.9 (d, *J* = 14.6 Hz, C—F), 120.3, 118.4 (d, *J* = 23.6 Hz, C—F, CH), 115.6 (d, *J* = 21.0 Hz, C—F, CH), 111.8 (CH), 108.1 (d, *J* = 26.7 Hz, C—F, CH), 61.0 (CH₂), 37.4 (d, *J* = 3.4 Hz, C—F, CH₂). Found: C, 59.60; H, 3.82; Cl, 7.96; F, 8.51; N, 12.58. Anal. calcd (%) for C₂₂H₁₇ClF₂N₄O₂: C, 59.67; H, 3.87; Cl, 8.00; F, 8.58; N, 12.65.

1-(2-(5-Fluoro-1-(6-chloro-2-fluorobenzyl)-2-oxoindolin-3-ylidene)hydrazinyl)-2-oxoethyl pyridin-1-iium chloride (5b**).** Yellow powder. Yield 83%, m.p. = 152–153 °C. IR spectrum, ν , cm^{−1}: 1355 (C—F), 1634 (C=C), 1687 (C=O), 3017 (CH), 3393 (NH). ¹H NMR (500 MHz, DMSO-*d*₆) δ 12.63 (s, 1H, NH), 9.10 (d, *J* = 6.1 Hz, 2H, Ar), 8.73 (t, *J* = 7.6 Hz, 1H, Ar), 8.27 (t, *J* = 6.8 Hz, 2H, Ar), 7.48–7.34 (m, 4H, Ar), 7.31–7.26 (m, 1H, Ar), 7.09–7.07 (m, 1H, Ar), 6.22 (s, 2H, CH₂), 5.15 (s, 2H, CH₂). ¹³C NMR (126 MHz, DMSO-*d*₆) δ 167.5, 163.5, 161.3 (d, *J* = 249.2 Hz, C—F), 158.6 (d, *J* = 239.8 Hz, C—F), 146.6 (CH), 146.5 (CH), 146.2, 139.4, 134.3 (d, *J* = 5.0 Hz, C—F, CH), 130.0 (d, *J* = 9.8 Hz, C—F, CH), 127.8 (CH), 127.7 (CH), 125.9 (d, *J* = 2.9 Hz, C—F), 120.2 (d, *J* = 16.5 Hz, C—F), 118.4 (d, *J* = 24.3 Hz, C—F, CH), 114.9 (d, *J* = 22.6 Hz, C—F, CH), 111.5 (d, *J* = 13.9 Hz, C—F), 108.1 (d, *J* = 2.3 Hz, C—F, CH), 61.1 (CH₂), 36.0 (d, *J* = 1.7 Hz, C—F, CH₂). Found: C, 55.30; H, 3.39; Cl, 14.79; F, 7.86; N, 11.70. Anal. calcd (%) for C₂₂H₁₆Cl₂F₂N₄O₂: C, 55.36; H, 3.38; Cl, 14.85; F, 7.96; N, 11.74.

1-(2-(5-Fluoro-2-oxo-1-(3-(trifluoromethyl)benzyl)indolin-3-ylidene)hydrazinyl)-2-oxoethyl pyridin-1-iium chloride (5c**).** Yellow powder. Yield 79%, m.p. = 172–173 °C. IR spectrum, ν , cm^{−1}: 1330 (C—F), 1637 (C=C), 1702 (C=O), 1680 (C=O), 3018 (CH), 3392 (NH).

¹H NMR (500 MHz, DMSO-*d*₆) δ 9.04 (d, *J* = 5.9 Hz, 2H, Ar), 8.71 (t, *J* = 7.8 Hz, 1H, Ar), 8.23 (t, *J* = 6.6 Hz, 2H, Ar), 7.74 (s, 1H, Ar), 7.68–7.65 (m, 2H, Ar), 7.61 (d, *J* = 7.8 Hz, 1H, Ar), 7.56–7.54 (m, 1H, Ar), 7.31–7.27 (m, 1H, Ar), 7.12 (dd, *J* = 8.8 Hz, *J* = 3.9 Hz, 1H, Ar), 6.16 (s, 2H, CH₂), 5.09 (s, 2H, CH₂). ¹³C NMR (126 MHz, DMSO-*d*₆) δ 168.0, 161.0, 159.2 (d, *J* = 239.8 Hz, C–F), 147.1 (CH), 146.7 (CH), 135.0, 131.8 (CH), 130.4 (CH), 129.9 (q, *J* = 31.7 Hz, C–F), 128.2 (CH), 125.0 (m, CH), 124.4 (m, CH), 124.2 (q, *J* = 272.4 Hz, C–F), 120.8, 118.8 (d, *J* = 23.7 Hz, C–F, CH), 112.2–121.1 (m, 2C, 2CH), 108.8 (d, *J* = 25.3 Hz, C–F, CH), 61.1 (CH₂), 42.7 (CH₂). ¹⁹F NMR (600 MHz, DMSO-*d*₆) δ –119.3, –61.0. Found: C, 56.00; H, 3.47; Cl, 7.17; F, 15.36; N, 11.38. Anal. calcd (%) for C₂₃H₁₇ClF₄N₄O₂: C, 56.05; H, 3.48; Cl, 7.19; F, 15.42; N, 11.37.

1-(2-(2-(5-Fluoro-2-oxo-1-((perfluorophenyl)methyl)indolin-3-ylidene)hydrazinyl)-2-oxoethyl)pyridin-1-ium chloride (**5d**). Yellow powder. Yield 72%, m.p. = 165–166 °C. IR spectrum, ν , cm^{−1}: 1337 (C–F), 1636 (C=C), 1707 (C=O), 1731 (C=O), 3030 (CH), 3402 (NH). ¹H NMR (600 MHz, DMSO-*d*₆) δ 12.59 (s, 1H, NH), 9.17–9.13 (m, 2H, Ar), 8.74 (t, *J* = 7.0 Hz, 1H, Ar), 8.28–8.26 (m, 2H, Ar), 7.51–7.48 (m, 1H, Ar), 7.43–7.40 (m, 1H, Ar), 7.30–7.28 (m, 1H, Ar), 6.26 (s, 2H, CH₂), 5.16 (s, 2H, CH₂). ¹³C NMR (151 MHz, DMSO-*d*₆) δ 167.7, 160.2, 158.7 (d, *J* = 239.8 Hz, C–F), 146.6 (CH), 146.5 (CH), 145.0 (dm, *J* = 248.2 Hz, C–F), 140.4 (dm, *J* = 252.0 Hz, C–F), 136.9 (dm, *J* = 249.4 Hz, C–F), 133.8, 127.6 (CH), 127.5 (d, *J* = 27.4 Hz, C–F, CH), 120.2, 118.5 (d, *J* = 24.0 Hz, C–F, CH), 111.6, 109.1, 107.9 (d, *J* = 26.1 Hz, C–F, CH), 61.0 (CH₂), 32.0 (CH₂). Found: C, 51.30; H, 2.50; Cl, 6.87; F, 22.08; N, 10.80. Anal. calcd (%) for C₂₂H₁₃ClF₆N₄O₂: C, 51.33; H, 2.55; Cl, 6.89; F, 22.14; N, 10.88.

1-(2-(2-(5-Methyl-2-oxo-1-(3-(trifluoromethyl)benzyl)indolin-3-ylidene)hydrazinyl)-2-oxoethyl)pyridin-1-ium chloride (**5e**). Yellow powder. Yield 85%, m.p. = 202–203 °C. IR spectrum, ν , cm^{−1}: 1375 (C–F), 1624 (C=C), 1688 (C=O), 3011 (CH), 3402 (NH). ¹H NMR (500 MHz, DMSO-*d*₆) δ 12.70 (s, 1H, NH), 9.14 (d, *J* = 5.7 Hz, 2H, Ar), 8.74 (t, *J* = 7.7 Hz, 1H, Ar), 8.28 (t, *J* = 7.2 Hz, 2H, Ar), 7.79 (s, 1H, Ar), 7.67–7.66 (m, 2H, Ar), 7.47 (s, 1H, Ar), 7.61 (d, *J* = 7.4 Hz, 1H, Ar), 7.47 (s, 1H, Ar), 7.28 (d, *J* = 7.3 Hz, 1H, Ar), 7.07 (d, *J* = 8.0 Hz, 1H, Ar), 6.25 (s, 2H, CH₂), 5.11 (s, 2H, CH₂), 2.33 (s, 3H, CH₃). ¹³C NMR (126 MHz, DMSO-*d*₆) δ 164.2, 163.9, 153.2, 146.6 (CH), 146.5 (CH), 140.8, 137.2, 135.2, 132.8 (CH), 132.5, 131.4, 129.8 (CH), 129.4 (q, *J* = 31.9 Hz, C–F), 127.7 (CH), 127.6 (CH), 124.4, 124.1 (CH), 124.0 (q, *J* = 273.9 Hz, C–F), 121.1, 110.4 (CH), 61.0 (CH₂), 42.2 (CH₂), 20.4 (CH₃). ¹⁹F NMR (600 MHz, DMSO-*d*₆) δ –61.0. Found: C, 58.90; H, 4.09; Cl, 7.27; F, 11.57; N, 11.43. Anal. calcd (%) for C₂₄H₂₀ClF₃N₄O₂: C, 58.96; H, 4.12; Cl, 7.25; F, 11.66; N, 11.46.

3.2. Biological Studies

3.2.1. Anticancer Activity

Cell Lines and Their Cultivation

Human cell cultures of tumor origin—HeLa (cervical tumor), HuTu 80 (human duodenal adenocarcinoma), ChangLiver (human liver HeLa-like line), and normal cell line WI38, VA 13 subline 2RA is a diploid human cell strain composed of fibroblasts derived from healthy lung tissue provided by The Gamaleya National Center for Epidemiology and Microbiology, as well as the Institute of Cytology of the Russian Academy of Sciences. They were grown in a nutrient medium DMEM (PanEco, Moscow, Russia) and MEM (PanEco, Moscow, Russia), containing fetal bovine serum (10% by volume) (ThermoFisher Scientific, Paisley, UK), Glutamax (2 mM) (Gibco, Scotland, UK), and penicillin-streptomycin (1% by volume) (PanEco, Moscow, Russia). The cultivation was carried out at 37 °C in a humidified CO₂ atmosphere (5%).

Determination of Cell Viability

Cell viability was determined by the MTT test [63]. Cells were seeded in a 96-well plate in the amount of 1 × 10⁴ cells/200 μL of complete nutrient medium and cultured at 37 °C in CO₂ (5%). After 24 h of incubation, various concentrations of test compounds in the range of 0.1 to 100 μM were added to the cell cultures, and then the cells were cultured

under the same conditions for 24 and 72 h. For each concentration, the experiment was carried out in triplicate.

All compounds were dissolved in DMSO and then diluted with the medium to the required concentration. The final content of DMSO in the well did not exceed 1% and did not have a toxic effect on the cells. The DMSO was also added to the control wells in a volume of 1%. After the incubation time, MTT (3-(4,5-dimethylthiazol-2-yl)-2,5-diphenyltetrazolium bromide, 5 mg/mL) was added to each well, and plates were additionally incubated for 2 h (until the characteristic color appeared).

Using a plate analyzer (Cytation3, BioTech Instruments Inc., Winooski, VT, USA), the optical density was determined at 530 nm. The concentration value causing 50% inhibition of cell population growth (IC_{50}) was determined from dose-dependent curves.

The IC_{50} parameter was calculated using the AAT Bioquest program [64].

The selectivity index (SI) is calculated as the ratio between the IC_{50} for normal cells and the IC_{50} for cancer cells [65].

Apoptosis

HuTu 80 cells at 1×10^6 cells/well in a final volume of 2 mL were seeded into six-well plates. After 24 h of incubation, various concentrations of tested compounds were added to the wells. The cells were harvested at 2757 g for 5 min and then washed twice with ice-cold PBS, followed by resuspension in binding buffer. Next, the samples were incubated with 5 μ L of annexin V-Alexa Fluor 647 (Sigma-Aldrich, Burlington, MA, USA) and 5 μ L of propidium iodide for 15 min at room temperature in the dark. Finally, the cells were analyzed by flow cytometry (Guava easyCyte, Merck, Rahway, NJ, USA) within 1 h. The experiments were repeated three times.

Mitochondrial Membrane Potential

To analyze the effect of compounds on changes in the mitochondrial membrane potential, we performed flow cytometry using JC-10 fluorescent dye (in the Mitochondria Membrane Potential Kit). In normal cells (with high membrane potential), JC-10 accumulates in the mitochondrial matrix, where it forms aggregates with red fluorescence. However, in apoptotic cells, JC-10 diffuses out of mitochondria, converts to its monomeric form, and emits green fluorescence, which is recorded by a flow cytometer [66]. Cells were harvested at 2757 g for 5 min and then washed twice with ice-cold PBS, followed by resuspension in JC-10 (10 μ g/mL) and incubation at 37 °C for 10 min. Then, the cells were rinsed three times and suspended in PBS, and the JC-10 fluorescence was observed by flow cytometry (Guava easyCyte, Merck, Rahway, NJ, USA).

ROS

HuTu 80 cells were incubated with tested compounds at concentrations of IC_{50} for 24 h. ROS generation was investigated using a flow cytometry assay and the CellROX® Deep Red flow cytometry kit. For this, HuTu 80 cells were harvested at 2000 rpm for 5 min and then washed twice with ice-cold PBS, followed by resuspension in 0.1 mL of medium without FBS, to which was added 0.2 μ L of CellROX® Deep Red and incubated at 37 °C for 30 min. After three times washing the cells and suspending them in PBS, the production of ROS in the cells was immediately monitored using a flow cytometer (Guava easyCyte, Merck, Rahway, NJ, USA).

Anticoagulant and Antiaggregation Activities Study

The in vitro experiments were performed using the blood of healthy male donors aged 18–24 years (a total of 54 donors). This study was approved by the Ethics Committee of the Federal State Budgetary Educational Institution of Higher Education at the Bashkir State Medical University of the Ministry of Health of the Russian Federation (No. 2, dated 17 October 2012). Informed consent was obtained from all participants before blood sampling. The blood was collected from the cubital vein using the vacuum blood collection

system BD Vacutainer® (Becton, Dickinson, and Company, Franklin Lakes, NJ, USA). A 3.8% sodium citrate solution in a 9:1 ratio was used as a venous blood stabilizer. The study of the effect on platelet aggregation was performed using the Born method [67] using the aggregometer «AT-02» (SPC Medtech, Moscow, Russia). The assessment of the antiplatelet activity of the studied compounds and reference preparations was started with a final concentration of 2×10^{-3} mol/L. Adenosine diphosphate (ADP; 20 µg/mL) and collagen (5 mg/mL) manufactured by Tehnologia-Standart Company, Barnaul, Russia, were used as inducers of aggregation. The study on the anticoagulant activity was performed by standard recognized clotting tests using the optical two-channel automatic analyzer of blood coagulation, Solar CGL 2110 (CJSC SOLAR, Minsk, Belarus). The following parameters were studied: activated partial thromboplastin time (APTT), prothrombin time (PT), and fibrinogen concentrations according to the Clauss method. The determination of the anticoagulant activity of the studied compounds and reference preparation was performed at a concentration of 5×10^{-4} g/mL using the reagents manufactured by Tehnologia-Standart Company (Barnaul, Russia). The results of the study were processed using the statistical package Statistica 10.0 (StatSoft Inc., Tulsa, OK, USA). The Shapiro-Wilk's test was used to check the normality of the actual dataset distribution. The form of distribution of the data obtained differed from the normal one; therefore, non-parametric methods were used for further analysis. The data were presented as medians and 25 and 75 percentiles. An analysis of variance was conducted using the Kruskal–Wallis test. A *p*-value of 0.05 was considered statistically significant.

3.2.2. Antiphytopathogenic Activity

Plant pathogenic bacterial strains *Micrococcus luteus* B-109, *Pectobacterium atrosepticum* 1043, *Pectobacterium carotovorum* subsp. *carotovorum* MI, *Pseudomonas fluorescens* EL-2.1, and *Xanthomonas campestris* B-610 and the fungal strain *Fusarium oxysporum* IBPPM 543 were from the Collection of Rhizosphere Microorganisms, IBPPM RAS (WFCC no. 975, WDCM no. 1021) (CM IBPPM, <http://collection.ibppm.ru>). The pathogenic fungus *Phytophthora cactorum* VKM F-985, provided by the All-Russian Collection of Microorganisms (VKM) and deposited at the A.E. Favorsky Irkutsk Institute of Chemistry, SB RAS, was also used as a test organism. Bacteria *M. luteus*, *P. carotovorum* subsp. *carotovorum*, *P. atrosepticum*, and *P. fluorescens* were grown in a meat–peptone medium (BP), and *X. campestris* was grown in the medium with glucose, yeast extract, and calcium carbonate (GYCa). Solid media contained Bacto agar (18 g/L); pH was adjusted to 7.2–7.4. All bacterial cultures were grown at 28 °C. The mycelial cultures of *F. oxysporum* and *P. cactorum* were grown on a glucose–peptone–yeast (GPY) nutrient medium at 27 °C. For inoculum preparation, both fungal strains were initially grown on the agar GPY in Petri dishes and then transferred into the seed medium by punching out 5 mm of the agar plate culture with a self-designed cutter.

The antibacterial and antifungal activities of the compounds were explored using the agar-well diffusion method and the technique of mycelial radial growth inhibition. The method of diffusion in agar (measuring the diameter of growth inhibition zones) was used to determine the bactericidal activity. The 6-mm wells were made in agar medium (GYCa for *Xanthomonas campestris* or BP for other bacteria). Bacterial suspensions were distributed over the agar surface, and the tested compound's solution (150 µL) was added to each well. The width of growth inhibition zones around the wells was determined after incubation for 36–40 h.

For the fungicidal activity analysis, radial growth (colony diameters) of the fungi on a solid medium in the absence and in the presence of the compounds **5a–e** and **7a–c** solutions at various concentrations were compared. The method consisted of the following: A sterile GPY agar medium (20.0 mL), which was melted and then allowed to cool to approximately 60 °C, was mixed with the precisely measured volumes of the solutions under question and poured into a sterile Petri dish (90 mm i.d.). After the solidification of GPY agar, the media were inoculated by the fungus using 10-day-old cultures of *F. oxysporum* or *P. cactorum*. The inoculation was conducted by transferring a 5-mm (i.d.) GPY-

agar block covered with mycelium to the center of the Petri dish, followed by incubation in a thermostat at 27 °C. The fungicidal effect was scored by the size of the mycelium colony on a Petri dish compared to the control without fungicidal admixtures to GPY agar. Each treatment was performed in at least four replicates in two independent experiments. The observation period ended when the control Petri dish was filled with mycelium (usually after 12 days). The inhibition of the phytopathogen colony growth by the compounds or the reference fungicide solutions was calculated as a percentage by which the mycelium radial propagation was decreased compared to the unaffected control; the latter was taken as 100% of growth (or zero percent of inhibition). The EC₅₀ value was calculated as the compound concentration at which the radial growth of the fungus colony was decreased by 50% relative to the non-fungicidal control. This effective concentration causing 50% of the fungal growth inhibition was determined from the dose-relative inhibition curves plotted for each tested compound. The solutions of the compounds were prepared with a concentration of 2 mmol/L (stock solution). For comparison, test compounds were also commonly applied as disinfecting agents, and antibiotics were used as a positive control.

3.2.3. Statistical Analysis

The data were expressed as the mean ± SEM. Statistical comparisons were made using one-way analysis of variance (ANOVA), followed by Dunnett's multiple comparison tests. Two-way repeated measures (mixed model) ANOVA followed by Bonferroni posttests were also used to compare the recognition of two objects. A difference with a *p*-value ≤ 0.05 was considered statistically significant. The statistical analysis was performed using GraphPad Prism 5 (GraphPad Software, San Diego, CA, USA).

4. Conclusions

A series of novel fluorinated 1-benzylisatins was synthesized with high yields by an easy one-pot reaction procedure. Using the acid-catalyzed reaction of new isatins with Girard's reagent P and its dimethyl analog, a wide range of water-soluble isatin-3-hydrazone were obtained. The most promising use of modified isatins as a basis for the creation of anticancer agents is possessed by ortho-substituted fluorine (**3a**), chlorine (**3b**), or both (**3d**) atoms in the benzyl fragment of the compound. The mechanism of the cytotoxic action of these substances is associated with apoptosis induction due to mitochondrial membrane dissipation and stimulation of reactive oxygen species production in tumor cells. It was shown that compounds **3a** and **3b** exhibit antiaggregation activity at the level of acetylsalicylic acid, and the whole series of fluorine-containing isatins does not adversely affect the hemostasis system as a whole. In a wide range of new water-soluble pyridinium isatin-3-acylhydrazone, substances **7c** and **5c,e** exhibit the highest activity. They have an antagonistic effect against phytopathogens of bacterial and fungal origin and can be considered biological preparations for combating plant diseases.

Supplementary Materials: The following supporting information can be downloaded at: <https://www.mdpi.com/article/10.3390/ijms242015119/s1>.

Author Contributions: A.V.B.—investigation (chemistry), writing—original draft preparation, and supervision (chemistry); I.A.L.—investigation (X-ray study); N.A.—investigation (chemistry); A.V., A.L., S.A., O.T., Z.V., A.V.S. and M.N.—investigation (in vitro study); R.Z.—funding acquisition; I.A.—project administration. All authors have read and agreed to the published version of the manuscript.

Funding: The synthesis: the studies of anticancer and antimicrobial activities were carried out at the Arbuzov Institute of Organic and Physical Chemistry and were supported by the Ministry of Science and Higher Education of the Russian Federation at the FRC Kazan Scientific Center (grant No. 075-15-2022-1128). The study of hemolytic activity was funded by the Non-Profit Joint-Stock Company "Korkyt Ata Kyzylorda University".

Institutional Review Board Statement: Not applicable.

Informed Consent Statement: Not applicable.

Data Availability Statement: Data is contained within the article.

Acknowledgments: The authors are grateful to the Assigned Spectral-Analytical Center of FRC Kazan Scientific Center of RAS for technical assistance in research. The evaluation of antiphytopathogenic activity (O.M.Tsivileva) was completed in the framework of theme No. 121031100266-3 of the Program of Fundamental Research of the Russian Academy of Sciences.

Conflicts of Interest: The authors declare no conflict of interest.

References

- Zhang, S.; Huang, D.; Wu, J.; Wang, Z. Decade Advance of Isatin in Three-component Reactions. *Asian J. Org. Chem.* **2023**, *12*, e202200591. [[CrossRef](#)]
- Pradeep, S.D.; Mohanan, P.V. Advancements in Schiff Bases of 1H-Indole-2,3-dione: A Versatile Heterocyclic Compound in Pharmacological Field. *Mini-Rev. Org. Chem.* **2023**, *20*, 45–54. [[CrossRef](#)]
- Efremov, A.M.; Beznos, O.V.; Eremeev, R.O.; Chesnokova, N.B.; Milaeva, E.R.; Shevtsova, E.F.; Lozinskaya, N.A. Microwave-Assisted Synthesis of 3-Hydroxy-2-oxindoles and Pilot Evaluation of Their Antiglaucomic Activity. *Int. J. Mol. Sci.* **2023**, *24*, 5101. [[CrossRef](#)]
- Nath, R.; Pathania, S.; Grover, G.; Akhtar, M. Isatin containing heterocycles for different biological activities: Analysis of structure activity relationship. *J. Mol. Struct.* **2020**, *1222*, 128900. [[CrossRef](#)]
- Gupta, A.K.; Tulsyan, S.; Bharadwaj, M.; Mehrotra, R. Systematic Review on Cytotoxic and Anticancer Potential of *N*-Substituted Isatins as Novel Class of Compounds Useful in Multidrug-Resistant Cancer Therapy: In Silico and In Vitro Analysis. *Top. Curr. Chem.* **2019**, *377*, 15. [[CrossRef](#)] [[PubMed](#)]
- Mushtaq, A.; Azam, U.; Mehreen, S.; Naseer, M.M. Synthetic α -glucosidase inhibitors as promising anti-diabetic agents: Recent developments and future challenges. *Eur. J. Med. Chem.* **2023**, *249*, 115119. [[CrossRef](#)] [[PubMed](#)]
- Cheke, R.S.; Firke, S.D.; Patila, R.R.; Bari, S.B. Isatin: New hope against convulsion. *Cent. Nerv. Syst. Agents Med. Chem.* **2018**, *18*, 76–101. [[CrossRef](#)]
- Saini, T.; Kumar, S.; Narasimhan, B. Central nervous system activities of Indole derivatives: An overview. *Cent. Nerv. Syst. Agents Med. Chem.* **2015**, *16*, 19–28. [[CrossRef](#)]
- Medvedev, A.; Igosheva, N.; Crumeyrolle-Arias, M.; Glover, V. Isatin: Role in stress and anxiety. *Stress* **2005**, *8*, 175–183. [[CrossRef](#)]
- Zhang, M.Z.; Chen, Q.; Yang, G.F. A review on recent developments of indole-containing antiviral agents. *Eur. J. Med. Chem.* **2015**, *89*, 421–441. [[CrossRef](#)]
- Bharathi Dileepan, A.G.; Daniel Prakash, T.; Ganesh Kumar, A.; Shameela Rajam, P.; Violet Dhayabaran, V.; Rajaram, R. Isatin based macrocyclic Schiff base ligands as novel candidates for antimicrobial and antioxidant drug design: In vitro DNA binding and biological studies. *J. Photochem. Photobiol. B Biol.* **2018**, *183*, 191–200. [[CrossRef](#)] [[PubMed](#)]
- Xu, Z.; Zhang, S.; Gao, C.; Fan, J.; Zhao, F.; Lv, Z.S.; Feng, L.S. Isatin hybrids and their anti-tuberculosis activity. *Chin. Chem. Lett.* **2017**, *28*, 159–167. [[CrossRef](#)]
- Raj, R.; Gut, J.; Rosenthal, P.J.; Kumar, V. 1H-1,2,3-triazole-tethered isatin-7-chloroquinoline and 3-hydroxy-indole-7-chloroquinoline conjugates: Synthesis and antimalarial evaluation. *Bioorg. Med. Chem. Lett.* **2014**, *24*, 756–759. [[CrossRef](#)] [[PubMed](#)]
- Rodríguez-Argüelles, M.C.; Cao, R.; García-Deibe, A.M.; Pelizzi, C.; Sanmartín-Matalobos, J.; Zani, F. Antibacterial and antifungal activity of metal(II) complexes of acylhydrazones of 3-isatin and 3-(N-methyl)isatin. *Polyhedron* **2009**, *28*, 2187–2195. [[CrossRef](#)]
- Guo, H. Isatin derivatives and their anti-bacterial activities. *Eur. J. Med. Chem.* **2019**, *164*, 678–688. [[CrossRef](#)]
- Ferraz de Paiva, R.E.; Vieira, E.G.; Rodrigues da Silva, D.; Wegermann, C.A.; Costa Ferreira, A.M. Anticancer Compounds Based on Isatin-Derivatives: Strategies to Ameliorate Selectivity and Efficiency. *Front. Mol. Biosci.* **2021**, *7*, 627272. [[CrossRef](#)]
- Rizzo, M.; Porta, C. Sunitinib in the treatment of renal cell carcinoma: An update on recent evidence. *Ther. Adv. Urol.* **2017**, *9*, 195–207. [[CrossRef](#)]
- Nadagouda, M.; Vijayasarathy, P.; Sin, A.; Nam, H.; Khan, S.; Parambath, J.B.M.; Mohamed, A.; Han, C. Antimicrobial activity of quaternary ammonium salts: Structure-activity relationship. *Med. Chem. Res.* **2022**, *31*, 1663–1678. [[CrossRef](#)]
- Dan, W.; Gao, J.; Qi, X.; Wang, J.; Dai, J. Antibacterial quaternary ammonium agents: Chemical diversity and biological mechanism. *Eur. J. Med. Chem.* **2022**, *243*, 114765. [[CrossRef](#)]
- Morrison, K.R.; Allen, R.A.; Minbiele, K.P.C.; Wuest, W.M. More QACs, more questions: Recent advances in structure activity relationships and hurdles in understanding resistance mechanisms. *Tetrahedron Lett.* **2019**, *60*, 150935. [[CrossRef](#)]
- Vereshchagin, A.N.; Frolov, N.A.; Egorova, K.S.; Seitkalieva, M.M.; Ananikov, V.P. Quaternary Ammonium Compounds (QACs) and Ionic Liquids (ILs) as Biocides: From Simple Antiseptics to Tunable Antimicrobials. *Int. J. Mol. Sci.* **2021**, *22*, 6793. [[CrossRef](#)] [[PubMed](#)]
- Sharma, V.D.; Aifuwa, E.O.; Heiney, P.A.; Ilies, M.A. Interfacial engineering of pyridinium gemini surfactants for the generation of synthetic transfection systems. *Biomaterials* **2013**, *34*, 6906–6921. [[CrossRef](#)] [[PubMed](#)]
- Pashirova, T.N.; Shaihutdinova, Z.M.; Vandyukov, A.E.; Voloshina, A.D.; Samorodov, A.V.; Pavlov, V.N.; Souto, E.B.; Mironov, V.F.; Bogdanov, A.V. Synthesis and structure-activity-toxicity relationships of DABCO containing ammonium amphiphiles based on natural isatin scaffold. *J. Mol. Liq.* **2022**, *365*, 120217. [[CrossRef](#)]

24. Chugunova, E.; Samsonov, V.; Gerasimova, T.; Rybalova, T.; Bagryanskaya, I. Synthesis and some properties of 2H-benzimidazole 1,3-dioxides. *Tetrahedron* **2015**, *71*, 7233–7244. [[CrossRef](#)]
25. Bogdanov, A.; Tsivileva, O.; Voloshina, A.; Lyubina, A.; Amerhanova, S.; Burtceva, E.; Bukharov, S.; Samorodov, A.; Pavlov, V. Synthesis and diverse biological activity profile of triethyl-ammonium isatin-3-hydrazone. *ADMET DMPK* **2022**, *10*, 163–179. [[CrossRef](#)]
26. Bogdanov, A.V.; Zaripova, I.F.; Voloshina, A.D.; Sapunova, A.S.; Kulik, N.V.; Tsivunina, I.V.; Dobrynin, A.B.; Mironov, V.F. Isatin derivatives bearing a fluorine atom. Part 1: Synthesis, hemotoxicity and antimicrobial activity evaluation of fluoro-benzylated water-soluble pyridinium isatin-3-acylhydrazones. *J. Fluor. Chem.* **2019**, *227*, 109345. [[CrossRef](#)]
27. Chugunova, E.A.; Akylbekov, N.I.; Appazov, N.O.; Makhrus, E.M.; Burilov, A.R. Synthesis of the First Tertiary Ammonium Derivative of 6-Chloro-5-nitrobenzofuroxan. *Russ. J. Org. Chem.* **2016**, *52*, 920–921. [[CrossRef](#)]
28. Zhou, Y.; Wang, J.; Gu, Z.; Wang, S.; Zhu, W.; Acena, J.L.; Soloshonok, V.A.; Izawa, K.; Liu, H. Next generation of fluorine-containing pharmaceuticals, compounds currently in phase II–III clinical trials of major pharmaceutical companies: New structural trends and therapeutic areas. *Chem. Rev.* **2016**, *116*, 422–518. [[CrossRef](#)]
29. Gillis, E.; Eastman, K.J.; Hill, M.D.; Donnelly, D.J.; Meanwell, N.A. Applications of fluorine in medicinal chemistry. *J. Med. Chem.* **2015**, *58*, 8315–8359. [[CrossRef](#)]
30. Haemmerle, M.; Stone, R.L.; Menter, D.G.; Afshar-Kharghan, V.; Sood, A.K. The Platelet Lifeline to Cancer: Challenges and Opportunities. *Cancer Cell* **2018**, *33*, 965–983. [[CrossRef](#)]
31. Morris, K.; Schnoor, B.; Papa, A.L. Platelet cancer cell interplay as a new therapeutic target. *Biochim. Biophys. Acta Rev. Cancer* **2022**, *1877*, 188770. [[CrossRef](#)]
32. Suzuki-Inoue, K. Platelets and cancer-associated thrombosis: Focusing on the platelet activation receptor CLEC-2 and podoplanin. *Blood* **2019**, *134*, 1912–1918. [[CrossRef](#)] [[PubMed](#)]
33. Tao, D.L.; Tassi Yunga, S.; Williams, C.D.; McCarty, O.J.T. Aspirin and antiplatelet treatments in cancer. *Blood* **2021**, *137*, 3201–3211. [[CrossRef](#)] [[PubMed](#)]
34. Xu, X.R.; Yousef, G.M.; Ni, H. Cancer and platelet crosstalk: Opportunities and challenges for aspirin and other antiplatelet agents. *Blood* **2018**, *131*, 1777–1789. [[CrossRef](#)]
35. Downer, M.; Allard, C.; Preston, M.; Gaziano, J.M.; Stampfer, M.J.; Mucci, L.A.; Batista, J.L. Regular aspirin use and the risk of lethal prostate cancer in the Physicians Health Study. *Eur. Urol.* **2017**, *72*, 821–827. [[CrossRef](#)]
36. Chen, W.Y.; Ballman, K.V.; Winer, E.P.; Openshaw, T.H.; Hahn, O.M.; Briccetti, F.M.; Johnson Irvin, W.; Pohlmann, P.R.; Carey, L.A.; Partridge, A.H.; et al. A randomised Phase III double-blinded placebo-controlled trial of aspirin as adjuvant therapy for breast cancer (A011502). *J. Clin. Oncol.* **2022**, *40*, 360922. [[CrossRef](#)]
37. Jafa, E.; Nisha, Y.; Kate, V.; Kayal, S.; Ganesh, R.N.; Sunitha, V.C.; Ganesan, P.; Penumadu, P.; Dubashi, B. Comparison of efficacy of aspirin plus EOX vs. EOX alone in patients with locally advanced and metastatic gastric cancer: A randomised clinical trial. *J. Gastrointest. Cancer* **2022**, *54*, 642–650. [[CrossRef](#)]
38. Pandey, V.K.; Dwivedi, A.; Pandey, O.P.; Sengupta, S.K. Organophosphorus Derivatives Containing Isatin-3-hydrazone as Chemotherapeuticants against Fungal Pathogens of Sugarcane. *J. Agric. Food Chem.* **2008**, *56*, 10779. [[CrossRef](#)]
39. Zampirolli, L.S.; de Lemos, M.J.; Goncalves, V.T.; de Souza, M.A.A.; de Souza, S.R.; Rumjanek, V.M.; DaCosta, J.B.N. Synthesis, characterization, and biological activity of a new class of dialkylphosphorylhydrazone derivatives of isatin. *Quim. Nova* **2014**, *37*, 989. [[CrossRef](#)]
40. Jothi Nayaki, S.; Ramya, R.; Srividhya, S.; Kiruthika, J.; Ramya, K.; Karthiga, S.; Arunachalam, M.; Kavitha, D. Antibacterial potentials of pillar[5]arene, pillar[4]arene[1]quinone derivative and their isatin inclusion complexes. *Supramol. Chem.* **2021**, *33*, 701–708. [[CrossRef](#)]
41. Abd-El-Khair, H.; Abdel-Gaied, T.G.; Mikhail, M.S.; Abdel-Alim, A.I.; El-Nasr, H.I.S. Biological control of *Pectobacterium carotovorum* subsp. *carotovorum*, the causal agent of bacterial soft rot in vegetables, in vitro and in vivo tests. *Bull. Natl. Res. Cent.* **2021**, *45*, 37. [[CrossRef](#)]
42. Huang, X.; Ren, J.; Li, P.; Feng, S.; Dong, P.; Ren, M. Potential of microbial endophytes to enhance the resistance to postharvest diseases of fruit and vegetables. *J. Sci. Food Agric.* **2021**, *101*, 1744–1757. [[CrossRef](#)] [[PubMed](#)]
43. Ragasova, L.; Penazova, E.; Gazdik, F.; Pecenka, J.; Cechova, J.; Pokluda, R.; Baranek, M.; Grzelbelus, D.; Eichmeier, A. The Change of Bacterial Spectrum after Storage of *X. campestris* pv. *campestris* Inoculated Cabbage Heads (*Brassica oleracea* var. *capitata* L.). *Agronomy* **2020**, *10*, 443. [[CrossRef](#)]
44. Erdrich, S.H.; Sharma, V.; Schurr, U.; Arsova, B.; Frunzke, J. Isolation of Novel *Xanthomonas* Phages Infecting the Plant Pathogens *X. translucens* and *X. campestris*. *Viruses* **2022**, *14*, 1449. [[CrossRef](#)]
45. Ray, M.; Ray, A.; Dash, S.; Mishra, A.; Achary, K.G.; Nayak, S.; Singh, S. Fungal disease detection in plants: Traditional assays, novel diagnostic techniques and biosensors. *Biosens. Bioelectron.* **2017**, *87*, 708–723. [[CrossRef](#)]
46. Wang, T.; Gao, C.; Cheng, Y.; Li, Z.; Chen, J.; Guo, L.; Xu, J. Molecular Diagnostics and Detection of Oomycetes on Fiber Crops. *Plants* **2020**, *9*, 769. [[CrossRef](#)]
47. Wang, L.; Wang, N.; Yu, J.; Wu, J.; Liu, H.; Lin, K.; Zhang, Y. Identification of Pathogens Causing Alfalfa Fusarium Root Rot in Inner Mongolia, China. *Agronomy* **2023**, *13*, 456. [[CrossRef](#)]
48. Alabugin, I.V.; Manoharan, M.; Peabody, S.; Weinhold, F. The Electronic Basis of Improper Hydrogen Bonding: A Subtle Balance of Hyperconjugation and Rehybridization. *J. Am. Chem. Soc.* **2003**, *125*, 5973–5987. [[CrossRef](#)]

49. Smolobochkin, A.V.; Gazizov, A.S.; Yakhshilikova, L.J.; Bekrenev, D.D.; Burilov, A.R.; Pudovik, M.A.; Lyubina, A.P.; Amerhanova, S.K.; Voloshina, A.D. Synthesis and Biological Evaluation of Taurine-Derived Diarylmethane and Dibenzoanthene Derivatives as Possible Cytotoxic and Antimicrobial Agents. *Chem. Biodivers.* **2022**, *19*, e202100970. [[CrossRef](#)]
50. Meier, P.; Finch, A.; Evan, G. Apoptosis in development. *Nature* **2000**, *407*, 796–801. [[CrossRef](#)]
51. Mironov, V.F.; Nemtarev, A.V.; Tsepaea, O.V.; Dimukhametov, M.N.; Litvinov, I.A.; Voloshina, A.D.; Pashirova, T.N.; Titov, E.A.; Lyubina, A.P.; Amerhanova, S.K.; et al. Rational Design 2-Hydroxypropylphosphonium Salts as Cancer Cell Mitochondria-Targeted Vectors: Synthesis, Structure, and Biological Properties. *Molecules* **2021**, *26*, 6350. [[CrossRef](#)] [[PubMed](#)]
52. Jia, Y.; Zhao, L. The antibacterial activity of fluoroquinolone derivatives: An update (2018–2021). *Eur. J. Med. Chem.* **2021**, *224*, 113741. [[CrossRef](#)] [[PubMed](#)]
53. Jiang, S.; Yang, G.; Shi, L.; Fan, L.; Pan, Z.; Wang, C.; Chang, X.; Zhou, B.; Xu, M.; Wu, L.; et al. Design, Catalyst-Free Synthesis of New Novel α -Trifluoromethylated Tertiary Alcohols Bearing Coumarins as Potential Antifungal Agents. *Molecules* **2023**, *28*, 260. [[CrossRef](#)] [[PubMed](#)]
54. Zhou, B.; Yuan, X.; Fan, L.; Pan, Z.; Chang, X.; Jiang, S.; Wu, L.; Wang, C.; Yang, G.; Ji, X.; et al. Synthesis and antifungal activities of novel trifluoroethane derivatives with coumarin, indole and thiophene. *J. Saudi Chem. Soc.* **2022**, *26*, 101572. [[CrossRef](#)]
55. Shi, Y.; Si, H.; Wang, P.; Chen, S.; Shang, S.; Song, Z.; Wang, Z.; Liao, S. Derivatization of Natural Compound β -Pinene Enhances Its In Vitro Antifungal Activity against Plant Pathogens. *Molecules* **2019**, *24*, 3144. [[CrossRef](#)] [[PubMed](#)]
56. Chudinova, E.M.; Platonov, V.A.; Alexandrova, A.V.; Elansky, S.N. Biology and resistance of phytopathogenic fungus Ilyonectria crassa to fungicides. *Plant Protect. News* **2020**, *103*, 192–196. [[CrossRef](#)]
57. Dubovoy, V.; Nawrocki, S.; Verma, G.; Wojtas, L.; Desai, P.; Al-Tameemi, H.; Brinzari, T.V.; Stranick, M.; Chen, D.; Xu, S.; et al. Synthesis, characterization, and investigation of the antimicrobial activity of cetylpyridinium tetrachlorozincate. *ACS Omega* **2020**, *5*, 10359–10365. [[CrossRef](#)]
58. Ardizzone, A.; Pericolini, E.; Paulone, S.; Orsi, C.F.; Castagnoli, A.; Oliva, I.; Strozzi, E.; Blasi, E. In vitro effects of commercial mouthwashes on several virulence traits of *Candida albicans*, *viridans streptococci* and *Enterococcus faecalis* colonizing the oral cavity. *PLoS ONE* **2018**, *13*, e0207262. [[CrossRef](#)]
59. Araujo, H.C.; Arias, L.S.; Caldeirão, A.C.M.; Assumpção, L.C.d.F.; Morceli, M.G.; de Souza Neto, F.N.; de Camargo, E.R.; Oliveira, S.H.P.; Pessan, J.P.; Monteiro, D.R. Novel Colloidal Nanocarrier of Cetylpyridinium Chloride: Antifungal Activities on *Candida* Species and Cytotoxic Potential on Murine Fibroblasts. *J. Fungi* **2020**, *6*, 218. [[CrossRef](#)]
60. APEX2 Version 2.1. *SAINTPlus. Data Reduction and Correction Program Version 7.31A*; Bruker Advanced X-ray Solutions; BrukerAXS Inc.: Madison, WI, USA, 2006.
61. Sheldrik, G.M. *SADABS, Program for Empirical X-ray Absorption Correction* (Bruker-Nonius, 1990–2004); University of Göttingen: Göttingen, Germany, 1996.
62. Sheldrick, G.M. A short history of SHELX. *Acta Crystallogr. Sect. C Struct. Chem.* **2015**, *71*, 3. [[CrossRef](#)]
63. Präbst, K.; Engelhardt, H.; Ringgeler, S.; Hübner, H. Basic Colorimetric Proliferation Assays: MTT, WST, and Resazurin. *Methods Mol. Biol.* **2017**, *1601*, 1–17. [[CrossRef](#)] [[PubMed](#)]
64. AAT Bioquest, Inc. Quest Graph™ IC50 Calculator. 17 March 2022. Available online: <https://www.aatbio.com/tools/ic50-calculator> (accessed on 16 September 2023).
65. Ayoub, M.; Wahby, Y.; Abdel-Hamid, H.; Ramadan, E.; Teleb, M.; Abu-Serie, M.; Noby, A. Design, synthesis and biological evaluation of novel a-acyloxy carboxamides via Passerini reaction as caspase 3/7 activators. *Eur. J. Med. Chem.* **2019**, *168*, 340–356. [[CrossRef](#)] [[PubMed](#)]
66. Andreeva, O.V.; Sapunova, A.S.; Lyubina, A.P.; Amerhanova, S.K.; Belenok, M.G.; Saifina, L.F.; Semenov, V.E.; Kataev, V.E. Synthesis, antimicrobial activity and cytotoxicity of triphenylphosphonium (TPP) conjugates of 1,2,3-triazolyl nucleoside analogues. *Bioorg. Chem.* **2021**, *116*, 105328. [[CrossRef](#)]
67. Born, G. Aggregation of blood platelets by adenosine diphosphate and its reversal. *Nature* **1962**, *194*, 927–929. [[CrossRef](#)] [[PubMed](#)]

Disclaimer/Publisher’s Note: The statements, opinions and data contained in all publications are solely those of the individual author(s) and contributor(s) and not of MDPI and/or the editor(s). MDPI and/or the editor(s) disclaim responsibility for any injury to people or property resulting from any ideas, methods, instructions or products referred to in the content.